ADDIS ABABA UNIVERSITY

ADDIS ABABA INSTITUTE OF TECHNOLOGY

SCHOOL OF CIVIL AND ENVIRONMENTAL ENGINEERING

Experimental Investigation of the Effect of Steel Slag Aggregate On the Bond Strength of Reinforced Concrete Member

---

A Thesis in Structural Engineering

By Melkam Gubay

March, 2022

Addis Ababa

A Thesis

Submitted in Partial Fulfillment of the Requirements for the Degree of Master of Science

The undersigned have examined the thesis entitled '**Experimental Investigation of the Effect of Steel Slag Aggregate on the Bond Strength of Reinforced Concrete Member**' presented by **Melkam Gubay**, a candidate for the degree of **Master of Science** and hereby certify that it is worthy of acceptance.

Dr. Abraham Gebre Advisor	Signature	March 04/2022 Date
Dr. Shifferaw Taye Internal Examiner	Signature	[illegible] March 2022 Date
Dr.- Ing. Bedilu Habte External Examiner	Signature	Feb 25/2022 Date
Dr.- Ing. Mebruk Mohammed Chair person	Signature	Date

UNDERTAKING

I certify that the research work titled "**Experimental Investigation of the Effect of Steel Slag Aggregate on the Bond Strength of Reinforced Concrete Member**" is my own work. The work has not been presented elsewhere for assessment. Where material used from other sources has been properly acknowledged / referred.

Melkam Gubay

Signature ____________

Date: March, 2022

III

ABSTRACT

The demand of concrete has increased due to expand of the construction industry. To protect the natural concrete making materials and to sustain the environment, reused of waste products as ingredients of concrete is becoming an inevitable option. From those Steel slag was selected due to its properties, which has almost similar properties to natural coarse aggregate, and it is easily accessible as a by-product from steel production industry. The mechanical property of the concrete with steel slag aggregate has been studied in different literatures. However, literature is limited on the bond behavior of steel slag concrete with steel bar. In this research, the effect of steel slag aggregate on the bond strength of reinforced concrete was investigated experimentally using cylindrical specimens (300 mm ×150 mm) with centrally embedded 12 mm, 14 mm and 16 mm deformed bar. The bond strength test was conducted with pullout test on short embedment length ($5d_b$) for 45 specimens. A total of five concrete mixes with 25% interval replacement of steel slag aggregate as coarse aggregate was carried out up to fully replaced for the normal strength concrete C-30. In addition to the bond strength test compressive and splitting tensile strength of the concrete were studied by using (150 mm size cube) and (300 ×150 mm) cylinder, respectively. Experimental test results shows that the compressive strength and splitting tensile strength of concrete increased up to 50% replacement of coarse aggregate by steel slag aggregate, and also the ultimate bond strength was increased up to 50% replacement. For all bar diameters, fully replaced steel slag aggregate concrete has compatible bond strength value with control concrete. On the other hand as the bar diameter increased the bond strength decreased due to the decrement of concrete cover. Additionally, this study proposed an empirical equation for ultimate bond strength based on the experimental results. ACI 318 and ESEN 1992 1 codes are more conservative and underestimated the bond strength values of all specimens.

Keywords: Steel Slag Aggregate, Bond Strength, Pullout Test, Bar Diameter

ACKNOWLEDGMENTS

Above all, I want to express my gratitude to the Almighty God for giving me the strength, and persistence to accomplish this thesis.

I would like to express my deepest gratitude and respect to my advisor Dr. Abrham Gebre, for his incredible support, motivation, supervision, and productive comments throughout the thesis. I am inspired by his commitment and research abilities.

And also I would like to express my great gratitude to Dr. Esayas Gebreyouhannes, for his humble treatment, helpful comments and suggestions.

I also extend my acknowledgment to Ing. Euyel, and Ing. Natnael for allowing me to use their pull-out machine for pull-out bond strength test.

Lastly, but not least, I would like to expand my heartfelt gratitude to all those who have directly and indirectly assisted me throughout my thesis research.

TABLE OF CONTENTS

LIST OF TABLES

LIST OF FIGURES

LIST OF ABBREVIATIONS

ACI	American Concrete Institute
CA	Coarse Aggregate
EAF	Electric Arc Furnace
FA	Fine Aggregate
FRP	Fiber Reinforced Polymer
OPC	Ordinary Portland cement
PVC	Polyvinyl Chloride conduit
RAC	Recycled Aggregate Concrete
RC	Reinforced Concrete
SSA	Steel Slag Aggregate

LIST OF SYMBOL

C	Cover thickness
s	Slip of reinforcement bar
d_b	Bar diameter
$f_c{}'$	Cylindrical compressive strength of the concrete
f_{ct}	Tensile strength of the concrete
f_y	Yield Strength of reinforcement bar
l_e	Embedment length
l_d	Development length
τ	Bond strength
τ_u	Ultimate bond strength
τ_f	Frictional bond resistance
$\tau_u{}^*$	Normalized bond strength

1. INTRODUCTION

1.1 Background

Concrete is a composite material composed of mainly of aggregate, cement and water. Due to the global demand of concrete is increased through time to time the requirement of ingredients also increased. And also aggregate is the main ingredient of concrete covering around three quarter volume of concrete matrix. Artificially generated aggregate and various industrial waste materials can be utilized as aggregate to decrease natural aggregate depletion. In Addition, the rapid growth of industrialization contributed to different types of waste by-products which are environmentally dangerous and creates problem in disposal. Hence, utilization of suitable waste by-products in construction industries has become an inevitable option in recent days [1]. The use of industrial waste as concrete aggregates offers a successful stage in the use of waste as an alternative to naturally available aggregates in the concrete production.

The sustainability goal, which drives the most of the current social challenges, asks for an increasingly re-use of wastes and by-products. Reusing recycled aggregates coming from the metallurgical industry, such as steel slag, could be a crucial approach for achieving both sustainability and mechanical/durability performance of concrete. This indicated that steel slag aggregate (SSA) has been found to be suitable for structural concrete production used as partially or fully replace of conventional coarse aggregate [2].

Steel slag is a by-product formed during the steel manufacturing process. It is the mainly composed of metal oxide and silicon oxide and it is very reactive aggregate. Normally, the use of steel slag for the concrete production reduces the need of natural rock as constructional material, hence preserving natural rock resources, maximum utilization and recycling of by-products. The utilization of those factory waste products used to recover the economy and to preserve the environment. The concrete containing the slag aggregate can have high strength and can be durable [3]. And also it is worth remembering the good results achieved on the electric arc furnace (EAF) slag RC beams subjected to gravity load, it shows an improvement of the ultimate capacity both flexure and shear failure [4]. On the other way the bond strength in between steel slag concrete and steel bar was also shows increment compare to the conventional concrete [5] within high strength concrete. Additionally, this paper studies the bond behavior of steel slag aggregate concrete with deformed steel bar for normal strength concrete.

In Reinforced Concrete (RC) structures, one of the causes of brittle failure is the sudden loss of bond between reinforcing bars and concrete in anchorage zones, which has been a leading cause of localized damage and even collapse of concrete structures. Bond refers to all mechanisms that allow stresses to be transmitted from steel reinforcement to the surrounding concrete, and it is one of the most significant properties of RC structures. In other words, bond in reinforced concrete is the resistance of surrounding concrete against pulling out of the reinforcing bars. The anchorage bond is developed to parallel to the direction of the force over the contact surface with the concrete in order to induced stress on rebar [6].

The bond strength of reinforced concrete is influenced by numerous factors: structural properties, bar and concrete properties. In addition, eccentricity, column axial load, and bond strength are the main factors that affect the RC joint performance. Therefore, it is important to discuss about the bond strength, which is a critical factor that affect joint strength. Many investigations on concrete structures have revealed that the bond stress between rebar and concrete is decreased at the beam-column joint [7].

1.2 Statement of Problem

Concrete is used extensively in infrastructure design and construction. Aggregates cover around 70% of the concrete volume. To reduce the shortage of natural aggregate and also to preserve the environment, researchers have given attention for the use of waste products in construction industry. Among the waste products, steel slag is almost non-recyclable and it has comparable property with conventional aggregate. And also the mechanical properties of the steel slag aggregate concrete are compatible compared with the corresponding control mixes [8]. Such promising results at material scale promoted the study development to the structural level like bond strength. The aggregate type, property and strength have a considerable effect on bond strength of the reinforced concrete structure. The effect of steel slag aggregate (SSA) on the bond strength between normal strength concrete and steel bar has not that much been studied yet. Therefore, the aim of this research is to study the bondage performance between steel slag aggregate concrete and steel bar to fulfill the gap.

1.3 Objective of the Study

1.3.1 General objective

The main objective of this experimental study is to examine the effect of steel slag aggregate which is used as coarse aggregate on bond strength of reinforced concrete.

1.3.2 Specific objectives

- To investigate the effect of steel slag aggregate on Compressive and Tensile strength of the concrete
- To investigate the effect steel slag aggregate on the bond strength of reinforced steel slag aggregate concrete
- To study the effect of bar diameter on the bond strength with steel slag aggregate concrete

1.4 Scope of the Study

This research is conducted by pullout test to examine the bond strength between Steel slag aggregate concrete and deformed steel bar. It also includes the compressive strength and splitting tensile strength test of the concrete. The specimens are prepared from control concrete with the target strength of C-30 and SSA concrete with (25%, 50%, 75% & 100%) of natural coarse aggregate replaced by steel slag aggregate. The bar diameter used for this study are 12, 14 and 16 mm. The other parameters are taken as constant.

1.5 Research Significant

Ethiopian Iron and steel factory’s solid waste (steel slag) is estimated about 3 tons /day. In contrast to other nations, steel slag is not widely used in the production of concrete in Ethiopia. Furthermore, factories incur significant expenses for the disposal of these waste products, which has a negative impact on the environment. From previous researchers’ reports show that steel slag has almost similar physical and chemical properties with conventional aggregate. Thus, it’s needed to examine the benefit of the steel slag for production of concrete as replacement of coarse aggregate and also other concrete making materials. The main consideration of this study is to save the natural aggregate and to preserve the environment by replacing the industrial waste products (SSA) as coarse aggregate. However, to use steel slag aggregate as natural coarse aggregate, its bond strength and engineering behavior needs investigation. So the influence of the SSA on the bond strength of reinforced concrete member is studied in this research.

1.6 Organization of the Thesis

This thesis is divided into five Chapters, each of which is well-organized as follows.

The first chapter of the thesis focuses on an introduction to the thesis, including the background of the study related with the steel slag aggregate and the bond strength, main objective, scope, and significant of the study. Chapter two covers the relevant literature, and several related publications in the field of study. The materials, techniques, and the experimental set-ups are presented in Chapter three. Chapter four provides the test results in detail, and also includes discussion of the test results. Finally, Chapter five presents conclusions and recommendations of the research.

2. LITERATURE REVIEW

2.1 Introduction

The literatures related with steel slag aggregate properties and its application on the concrete production, bond strength and bond testing techniques, bond-slip relation and empirical equations of bond strength are discussed in this portion.

2.2 Steel Slag Aggregate on the Concrete Production

Conventionally concrete is proper mixture of cement, aggregate and water. Due to demand of concrete is increased, producing novel concrete by using the recycled materials is increased. And also aggregates occupy almost 70-75 percent of the total volume of concrete. So it is necessary to use an alternative material in construction which could use as replacing the natural aggregate without affecting the property of fresh and harden concrete. In this regard, many researchers have given their attention on by-products coming from metallurgical factory [9]. The industrial wastes such as steel slag are used as an alternative construction material to produce concrete as partially of fully replacing the aggregate.

Steel Slag

Steel slag is a waste product generated during the purification and alloying of pig iron and steel. Slag is produced at two stages during the manufacturing process of steel. The metal ore is heated to a high temperature in the first phase to identify impurities. Those impurities separated and then poured out of the top section of melted metal scraps as a waste product called steel slag. On further processing of metal like casting and alloying different substances are added to purify the steel, on thus process also slag is produced as the waste [10]. The production of iron and steel as well as the process of steel slag production is shown on Figure 2.1 below.

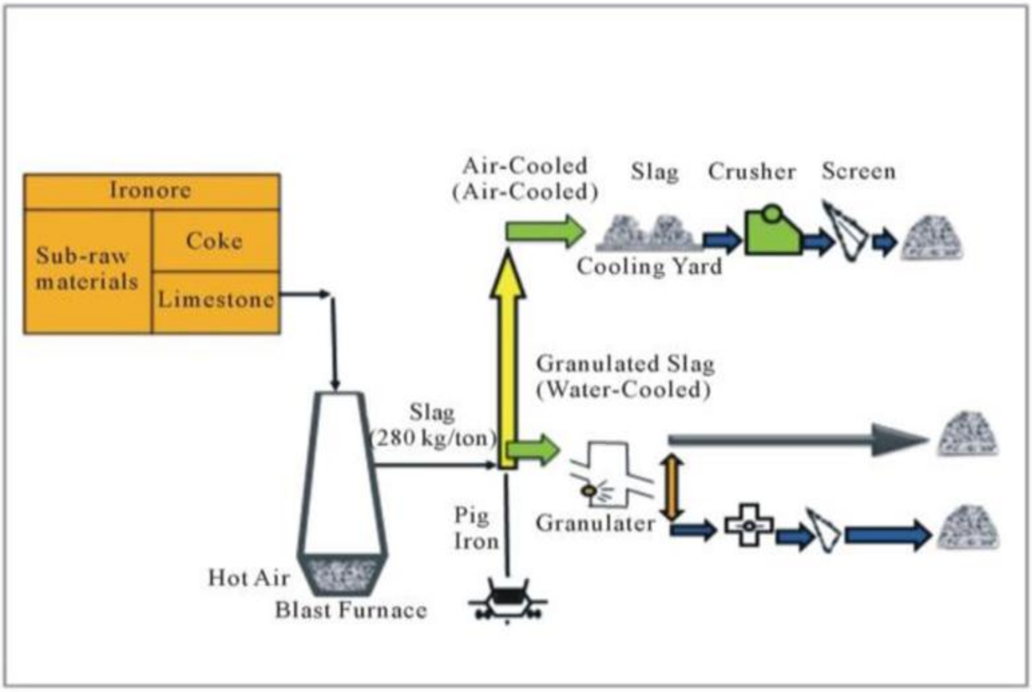

Figure 2.1. Flowchart of blast furnace operation [10]

Steel slag is a key byproduct of steelmaking process. And also steel slag is divided into two types: black basic slag, which has a lime content of less than 40%, generated from cold loading of scrap; and white basic slag, with lime content greater than 40%, produced during grinding, when more lime is added to remove sulfur and phosphorus from the produced steel [11]. Steel slag's physical and chemical properties are influenced by type of steel furnace, steel manufacturing plant, and slag processing. Additionally, the chemical composition of steel slag largely depends on melting and cooling processes.

Mechanical Property of Concrete with Steel Slag Aggregate

As discussed by Padmapriya, R. et al [9], steel slag aggregate has almost similar physical properties and chemical property with the natural aggregate. And also the partially and fully replacement of steel slag aggregate for concrete production has improved the mechanical property of the concrete within different grade of concrete. For normal strength of concrete, the mechanical property of the concrete increases up to 40 percent replacement of coarse aggregate. It was observed that an improvement of the compressive strength by 27.02%. The shape and surface texture of SSA have a significant role on the improvement of mechanical property of concrete’s, which improve aggregate-cement matrix adhesion. On the other hand steel slag is light weight compared to natural aggregate, and the density of the concrete is lower than the conventional aggregate concrete. This is a major advantage by decreasing the self-weight of concrete [12].

Devi, V.S. and Gnanavel, B.K. [13] studied that steel slag is utilized to partially substitute fine and coarse aggregate in the production of concrete. The workability of the concrete decreased as the percentage of replacement increased from 0% to 50%. However, the mechanical properties of the concrete, such as compressive strength, splitting tensile strength, and durability, indicate an increase of up to 30% and 40% in coarse and fine aggregate replacement, respectively. By adding steel slag either as fine aggregate or coarse aggregate, obtained better acid resistance than natural aggregate.

According to Warudkar, A.A. and Nigade, Y.M. [14], it was discovered that the compressive strength of normal strength concrete rises with increasing steel slag substitution up to 75% of natural coarse aggregate, but decreases after that. The compressive strength of the concrete was increased by 14% for 75% of natural coarse aggregate replaced by steel slag. The concrete's splitting tensile strength and flexural strength were both increased up to 75%, with the flexural strength increasing the most from 4.47 to 5.16 MPa. It shows that 15.43% increases compared with control concrete. In addition, the acid and sulphate resistance of steel slag aggregate concrete was higher than that of conventional concrete.

If study by Van Tran, M. et al [15] shows that the compressive strength of the high strength concrete enhanced as the basalt coarse aggregate was fully replaced by steel slag aggregate, and with an increase of steel slag aggregate percentage in the overall aggregate content. With the full basalt coarse aggregate, the steel slag aggregate increased the concrete compressive strength about 5% to 17% at varied w/c ratios. And also the unit weight of concrete made with steel slag coarse aggregate was substantially greater than that of concrete made with basalt coarse aggregate. In terms of chloride penetration resistance, concrete cast with steel aggregate was more durable than concrete cast with natural basalt aggregate.

Additionally, Faleschini, F. et al [16] described that substituting granite coarse aggregate with steel slag aggregate in concrete improves compressive strength when the replacement level is up to 100% for high strength concrete. When steel slag is used instead of natural aggregate, the split tensile strength and flexural strength are at their highest. Steel slag aggregate replaces granite coarse aggregate in concrete, improving its mechanical properties.

Bond Behavior of Reinforced Concrete with Steel Slag Aggregate

Bond strength is the measure of the effectiveness of the grip between the reinforcement bar and the concrete surface. The bond strength of reinforced concrete member is affected by bar diameter, embedment length of bar, bar rip arrangement, concrete cover, concrete strength, aggregate type and strength and slump and workability of concrete [17]. Whereas, concrete is a composite material and the strength of concrete is determined by the behavior of its ingredients. Cement, aggregates, and water are the three main elements of concrete. Depending on the mix proportions aggregate is the main ingredient of concrete. However, a closer look indicates that the qualities of aggregates have an impact on the properties of both hardened and fresh concrete. Aggregate types and properties have a direct impact on concrete strength, which in turn has an impact on bond strength. For the structural application of recycled aggregate concrete (RAC) like steel slag aggregate concrete, the bond characteristics of reinforcing bars with embedded in RAC needs attention on the bond between the rebar and the surrounding concrete.

According to Faleschini, F. et al [5], the bond behavior of reinforcement bar and EAF slag compared to conventional aggregate concrete on high strength concrete, an increase in bond stress was noticed on the specimens with EAF slag concrete. The highest bond strength is observed in specimens including EAF slag, with an increase of 41% and 30% in the peak stress, if compared respectively to round and crushed natural aggregate concrete mixture.

2.3 Bond Strength

Reinforced concrete is made up of brittle concrete that is strong in compression with reinforcing steel that is strong and ductile in tension. Maintaining composite action requires a transfer of the load in between steel bar and concrete. Bond is the term for the load transmission that results in an idealized continuous stress field along the steel-concrete interface. One of the most significant aspects of RC structure is bond, which refers to all of the systems that allows axial forces to be transferred from the steel bar to the embedding concrete. It is the measure of interaction between the rebar and the concrete it is expressed by bond stress [18]. It is an important parameter and greatly affects the joint behavior. To avoid a significant slip occurrence between the concrete and steel bar the bond must be durable.

2.3.1 Bond Strength Test Methods

Pullout specimens, beam-end specimens, beam anchorage specimens, and splice specimens are the four most typical bond strength test setups. Because of the simplicity of testing and producing the specimens, the direct pullout test is one of the most commonly used bond strength test method [7].

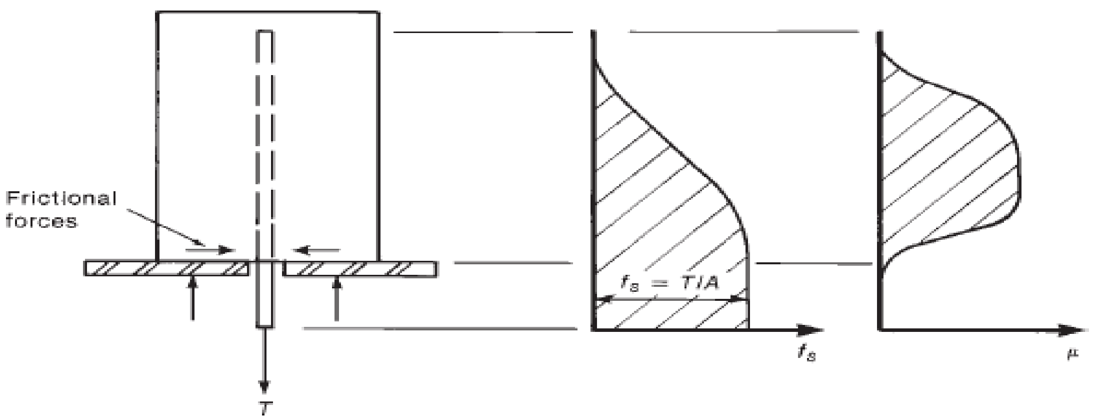

a). Testing method **(b). Steel bar stress** **(c). Bond stress**

Figure 2.2. Pull-out test bond stress distribution diagram [19]

2.4 Bond-Slip Relationship

As presented by Shima, H. et al [20], the bond action between the steel bar and the concrete is often considered by using the bold-slip relation. The bond-slip relation were different for various bond test types such as pullout test for shorter specimen and beam end test the longer one. The bond stress distribution along the bar was calculated from the stress-slip distribution. Slip is the displacement of the bar at the point from the fixed point of the concrete. It is usually measured by transducer during the bond strength test.

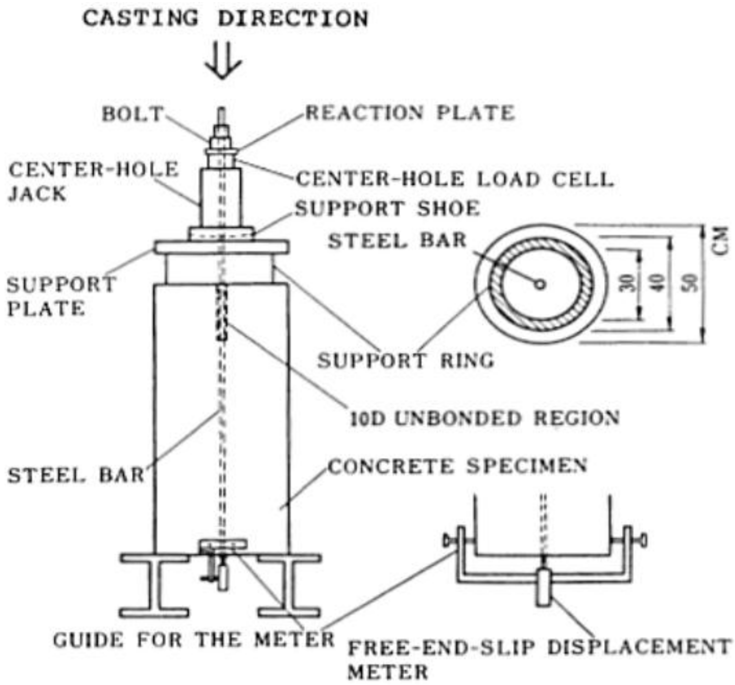

Figure 2.3. Specimen and instruments for pullout test [20]

The slope of the steel bar stress distribution curve at every position on an embedded bar is proportional to the local bond stress. At any point, the bond stress τ is defined as

$$\tau = \frac{Dd\sigma}{4dx} \qquad (2.1)$$

Where

D is the bar diameter

$\frac{d\sigma}{dx}$ is the slope of the stress -slip distribution curve

The bond behavior of reinforced concrete member is commonly described by the relation of stress with slip. The Bond-slip relationship is as shown in Figure 2.4 for splitting and pullout failure [21].

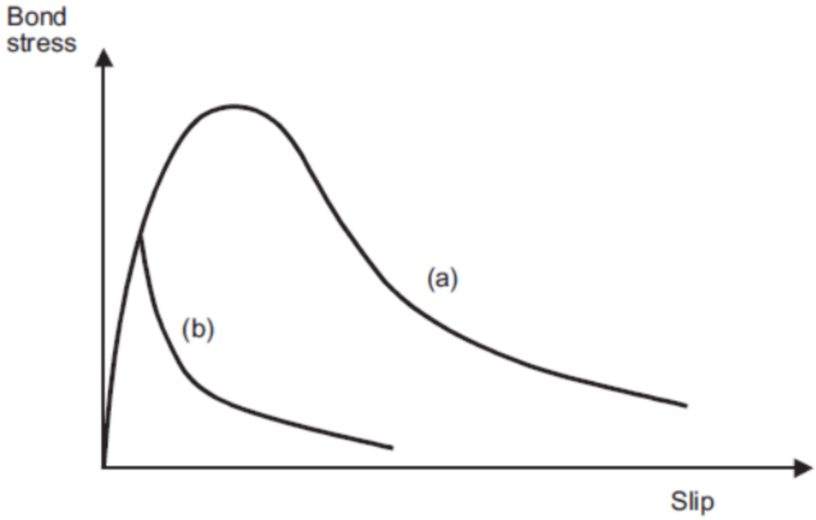

Figure 2.4. (a) Pull-out failure, (b) Splitting failure, or loss of bond due to Yielding of the reinforcement

2.5 Bond-Slip Model

Bond stress is the mechanical instruction in between steel and concrete. In structural design, the scholars use the simplified calculation of the average bond stress to represent the bond strength of steel bar with the concrete. Eligehausen, R. et al. [22] set the shorter embedment length l_e ($l_e < 5d_b$, l_e is the embedment length and d_b is bar diameter). The shorter embedment length is intended to reduce the influence of uneven bond stress distribution, and the experiment's outcome may be near to the real local bond stress.

With increasing load cycles, the values of residual slip and load increased, however at the peak point, repeated load had little effect on bond stress and slip [23].

The differential equation for bond stress on evenly distributed bond stress along the anchoring length [24].

$$\Delta F = \frac{\pi d_b^2}{4} d\sigma_s = \tau \pi d_b dx \tag{2.2}$$

Where

τ is the bond strength

d_b is bar diameter and

σ_s is the stress of reinforcing bar

The bond stress derivation formula became

$$\tau(x) = \frac{\Delta F}{\pi d_b \Delta x} = \frac{d_b}{4}\frac{d\sigma_s}{dx} \quad (2.3)$$

Numerous factors influence the bond stress-slip relationship, including bar type (plain and deformed), bar rib shape, concrete compressive and splitting tensile strength, concrete cover thickness, and bar location at the moment of casting. Figure 2.5 shows bond stress-slip relationship for deformed bars in the elastic range [25].

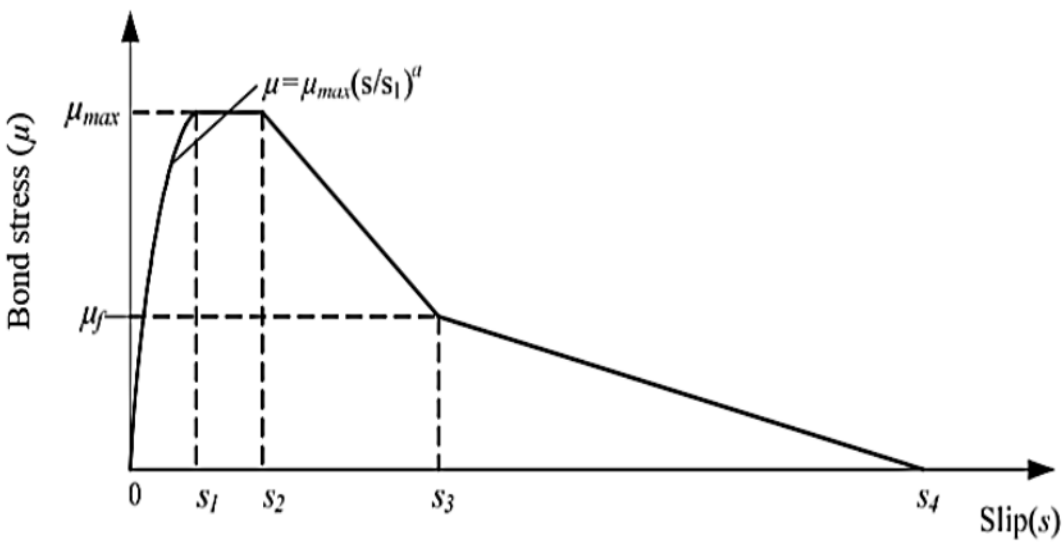

Figure 2.5. Bond stress -slip relation curve

Bond behavior between the steel bar and concrete has been investigated by many researchers. The CEB FIP model code 2010 [26] has been described the bond slip mechanism with the failure mode as showed in Figure 2.6. For pull out failure, non-linear ascending branch is proposed and followed by constant linear stage and simplified linear descending. For splitting failure, the model reduced to non-linear ascending branch and simplified linear descending branch.

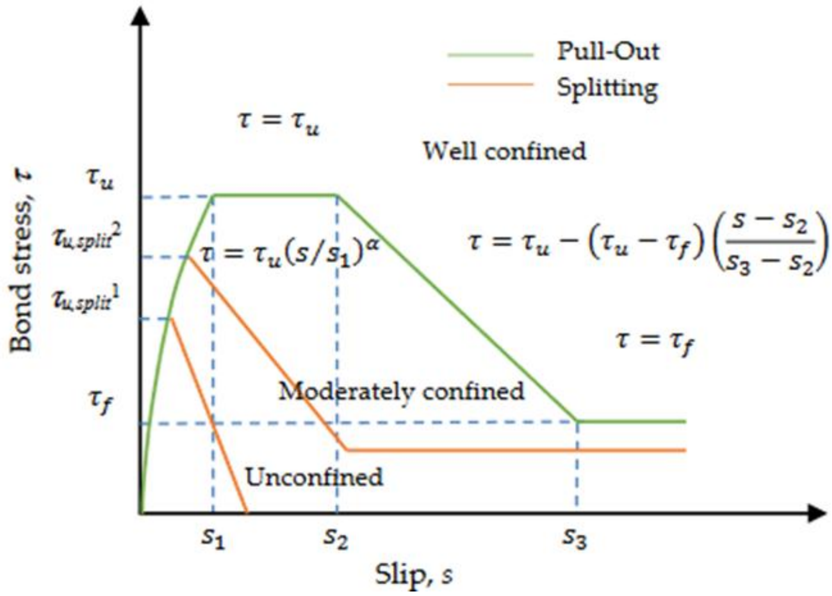

Figure 2.6. Analytical bond stress–slip relationship

According to CEB FIP Model Code [26], the rising branch refers to the stage where the reinforcement ribs penetrate into the concrete mortal matrix, causing local crushing and micro-cracking. Hence, the bond stress increases nonlinearly in ascending branch until the slip S equals S_1 (equation 2.4). The horizontal line between S_1 and S_2 occurs only for well-confined concrete as described by (equation 2.5). There is a steady and maximum bond stress throughout this stage. The descending branch refers to the weakening of the connection caused by concrete cracking along the rebar (equation 2.6). The remaining bond capacity is residual bond represented by the last horizontal line, which is maintained by the minimum transverse reinforcement (equation 2.7).

$$\tau = \tau_u \left(\frac{s}{s_1}\right)^\alpha \qquad \text{for } 0 \leq s \leq s \qquad (2.4)$$

$$\tau = \tau_u \qquad \text{for } s_1 \leq s \leq s_2 \qquad (2.5)$$

$$\tau = \tau_u - (\tau_u - \tau_f)\left(\frac{s - s_2}{s_3 - s_2}\right) \qquad \text{for } s_2 \leq s \leq s_3 \qquad (2.6)$$

$$\tau = \tau_f \qquad \text{for } s > s_3 \qquad (2.7)$$

2.6 Bond-Slip Mechanics

A shear stress is transferred along the steel-concrete interaction and is known as the bond stress. The stress transfer capacity of the deformed steel bar-concrete interface is primarily made up of three resistance transfer machines. Those are as shows on Figure

2.7 [7, 27] chemical adhesion between steel bar and concrete, friction between the two surfaces, and mechanical interlock of the ribs against the concrete. When the chemical adhesion was departed, the embedded rebar began to slip; and the mechanism of stress transfer relied mostly on sliding friction. Finally, as the slip of steel bar increased the mechanical interlocking cannot resist the applied load and the load significantly decreased, and slip is raised.

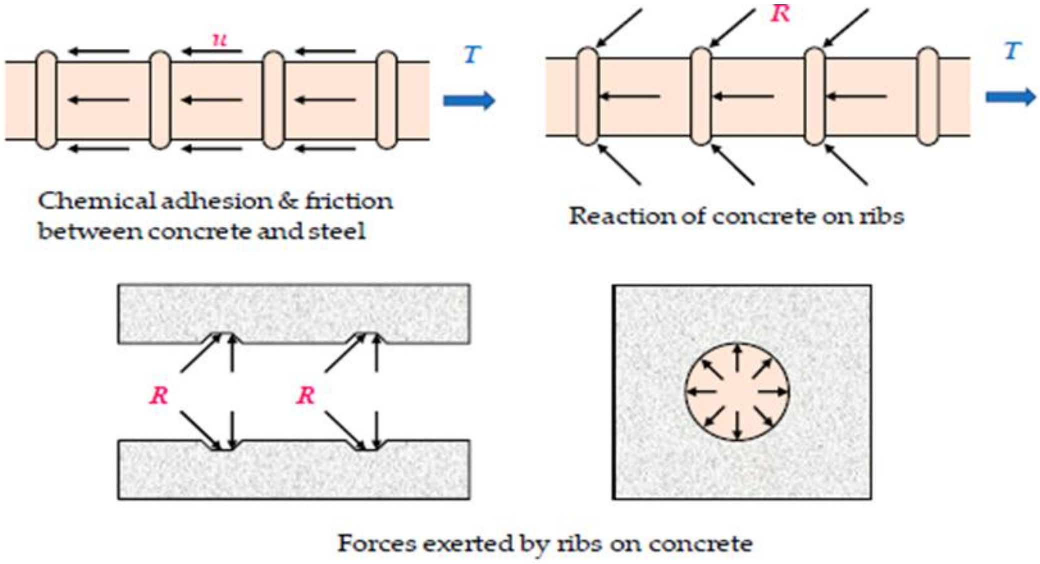

Figure 2.7. Transfer mechanisms of bond force

Friction and chemical adhesion have a big role in the bond strength of plain bars; however the bond strength of deformed bars is primarily determined by mechanical bearing capability. On the un-deformed part of the reinforcing bar, adhesion is the stick-like bond between the steel and the concrete. Bearing resistance is the force exerted by the concrete against the deformation of the steel bar [28]. Figure 2.8 shows the three primary bond-slip mechanisms between reinforced bar and concrete.

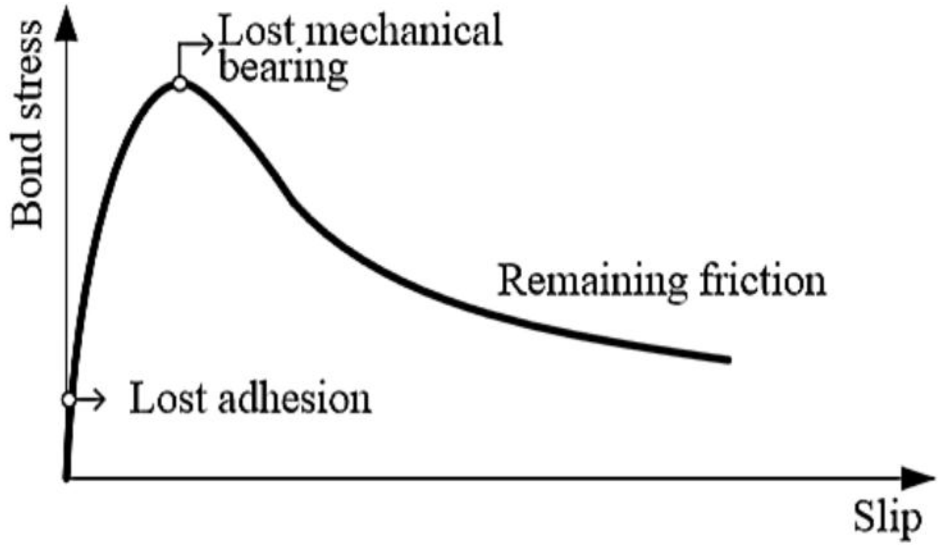

Figure 2.8. Bond stress-slip mechanism of load transfer [28]

2.6.1 Failure Mode of the Bond Strength

Pull-out failure, splitting failure, and yielding failure of steel bars are the three most prevalent bond strength failure modes. The steel bar was pulled out from the embedded concrete during the pull-out failure mode. This failure mode is typical in plain bar pull-out tests of concrete member. And also splitting failure is commonly occurred on deformed steel bars. The radial component of the squeeze force of the steel deformed rib on the concrete would cause circumferential tension in the surrounding concrete, and if this force was larger than the tensile strength of concrete, the concrete cover would be split. Yielding failure of the steel bar referred to the failure mode where the steel bar was yielded before the bond strength between the steel bar and the concrete was exceeded [21].

The degree of confinement, which is expressed in the amount of transverse reinforcement or sufficient concrete cover, determines the bond failure mode. Transverse reinforcement and/or extra concrete surrounding provide confinement which reducing tensile stresses below the tensile modulus of rupture. As a result, pull out failure would occur in well-confined RC members, similar to the confined part of beam-column joints [22,29] unless there is no sufficient confinement provided to resist the tensile forces the bond strength is fail by splitting failure.

2.7 Factors affecting Bond Strength

The main factors that affect the bond strength of deformed bars with concrete includes development length of bar, bar size and surface conditions, concrete cover, concrete strength, confinement of concrete (due to transverse reinforcement and FRP), position of the bars during concrete casting, aggregates size and strength and concrete workability ACI Committee 408, 2003 [7].

2.7.1 Development length of bar

The bond capacity increases as the bar's development length increases. This increase is linear but not proportional to the length due to the non-uniform nature of bond forces. The loaded end of the bonded length transfers the most of the bond forces to the concrete in splice and pullout specimens. The bonding force is transferred with little effect by the non-loaded or free end. When a splitting failure happens, a fracture appears on the concrete's surface. The energy needed to initiate the crack increases with an increase of the bonded length but at a slower rate [7].

2.7.2 Bar Size

The relation between bond strength and bar size isn't usually valued. The reason for this is because (1) the size of the bar rises the longer development or splice length required, and (2) larger bars generate higher total bond force for a given development length than smaller bars for the same degree of confinement. For a larger bar to properly develop a given bar stress, a longer development length is required (the first point). To start with the second issue, longer bars require more bond force to create a splitting or pullout failure for a given bonded length [7]. Smaller bars appear to have a greater advantage when measured in terms of bond stress; thus, conventional wisdom suggests that it is preferable to use a large number of small bars rather than a small number of large bars; this is true until bar spacing is reduced to the point where bond strength is reduced [30, 31]. Therefore, it is preferable to use smaller size bars than larger bars having the same area.

2.7.3 Concrete cover and bar spacing

The larger the bar spacing and cover the better the bond strength until another failure mode is prompted. Pull-out failure or a failure by yielding of the bar can be expected if the cover and/or bar spacing are too large, instead of the splitting failure that occurs when the cover and/or the bar spacing is small. Splitting failures usually appear in the smallest of covers. If a bond fails in most structures, it is usually due to splitting [7].

2.7.4 Concrete strength

The tensile strength of the concrete determines the bond force between the steel bars and the concrete. The bond strength typically has been calculated as $(f_c')^{1/2}$ where f_c' is the concrete's compressive strength. This is because of the square root of the concrete compressive strength is exactly related to the tensile strength of the concrete. Recent researches on bond strength, however, have demonstrated that equating bond strength to $(f_c')^{1/4}$ provide a more accurate depiction. This is due to the fact that, in addition to the concrete tensile strength, the bond strength is determined by the concrete fracture energy [7]. When the loading energy exceeds the concrete fracture energy, concrete cracks formed. Those cracks would decrease the bond between the steel bars and the concrete. Therefore, the higher the fracture energy is, the higher the bond strength. In general, it has been found that as the concrete strength increases, the bond strength increases but at a slower rate.

Iqbal, S. et al [32] studied the effect of maximum aggregate size (25.4mm, 19.05mm, 12.7mm and 9.53mm) on bond strength of reinforced concrete. The result shows that, as the maximum aggregate size increased the compressive strength and splitting tensile strength of concrete decreased. The bond strength of concrete does not change when the maximum aggregate size of coarse aggregates is greater than 10mm, while it decreases when the maximum aggregate size is less than 10mm. This might be due to smaller aggregates providing less locking to the pulled out bar.

2.8 Bond Stress Equations in Code provisions and Empirical Equations

Bond stress is evaluated using several bond strength tests, such as the RILEM pull-out test [33], which is a standardized test with a short embedment length. Pullout specimens have a short bond length ($5d_b$), which is supposed to represent the actual bond stress.

In addition, CEB-FIP 2010 model code [26] recommends a minimum cross section of embedded concrete of the steel bar to avoid early bond failure due to splitting of the concrete cover.

The average bond stress can be determined by dividing the pullout tensile load to the rebar's embedded surface area, which is

$$\tau = \frac{P}{\pi d_b l_e} \qquad (2.8)$$

The average bond stress is multiplied by the embedded steel bar area to get the tensile pull-out load, as shown below:

$$P = \tau A \qquad (2.9)$$

Where

P is pullout tensile force

d_b is bar diameter

l_e is embedment length

A is area of embedded rebar

Equations in Code provisions

Various codes have provided different equations for calculating the bond stress between steel rebar and concrete, taking into account various factors such as compressive strength, embedded length, bar diameter, and concrete cover thickness.

Ethiopian Building Code

The Ethiopian building code (ESEN 1992 1-1:2015) [34] has specified an equation for the ultimate bond strength as following

$$f_{bd} = 2.25\eta_1\eta_2 f_{ctd} \qquad (2.10)$$

Where

f_{ctd} is the design concrete tensile strength , $f_{ctd} = \frac{\alpha_{ct} f_{ctk0.05}}{\gamma_c}$

η_1 is a associated with the quality bond condition and bar position during casting

η_2 is associated with diameter of bar

American Concrete Institute (ACI) 318 code [35] forwards an equation to determine the minimum bond stress, which is considered long development length as given below:

$$\tau = \frac{f_y A_b}{\pi d_b l_d} \qquad (2.11)$$

Where

f_y is steel bar yield strength

A_b is rebar area

d_b is bar diameter

l_d is development length

The development length (l_d) for No. 19 and smaller deformed bars is determined by using the (ACI) 318 code [34] which is in tension as follow:

$$l_d = \left(\frac{f_y \psi_e \psi_t \psi_s \lambda}{2.1 \sqrt{f_c'} {d_b}^2} \right) d_b \quad (2.12)$$

Where

ψt is the location factor

ψe is the coating factor

ψs is the reinforcement size factor

λ is the type of concrete

f_y is yield strength of rebar

f_c' is cylindrical compressive strength of the concrete in MPa

d_b is bar diameter

CEB-FIP Model Code 2010 [26] provided bond strength equation for the specimens with good confinement and non-split failure as follows:

$$\tau_u = 2.5 \sqrt{f_c'} \quad (2.13)$$

Huang et al. model code [25] forward the prediction formula to calculate the bond stress as shown below:

$$\tau_u = 0.45 f_c' \quad (2.14)$$

Empirical Equations

Several investigators have proposed empirical equation that used to determine bond stress such like:

Shima, H. et al. (1987) [20] represent the bond models and proposed the empirical equation for the long embedment length of bar. The concrete strength and diameter of bar were the main parameters to predict the bond-slip relationship.

$$\tau = 0.9{f_c'}^{\frac{2}{3}}\left(1 - e^{-40\left(\frac{s}{d_b}\right)^{0.6}}\right) \tag{2.15}$$

Where

τ is bond stress in MPa,

f_c' is cylindrical compressive strength of the concrete

d_b is bar diameter

s is slip

Orangun, C.O. et al. (1977) [36] forwarded an equation for ultimate bond stress as:

$$\tau_u = 0.083035\sqrt{f_c'}\left(1.2 + 3\frac{C}{d_b} + 50\frac{d_b}{l_d}\right) \tag{2.16}$$

Where

C is the minimum concrete cover

l_d is the development length

Darwin, D. et al. (1992) [37] suggested an empirical equation for ultimate bond stress as:

$$\tau_u = 0.083035\sqrt{f_c'}\left(6.67\left(0.5 + \frac{C_{min}}{d_b}\right)\left(0.92 + 0.08\frac{C_{max}}{C_{min}}\right) + 235.62\frac{d_b}{l_d}\right) \tag{2.17}$$

Where

C_{min} = minimum (C_s, C_b, $C_s/2$), C_{max} = maximum (min (C_s, $C_{si}/2$), C_b)

C_{si} is the bar spacing

C_s is the side cover, and

C_b is the bottom cover

Chapman, R.A. and Shah, S.P. (1987) [38] conducted an experimental investigation for the assessment of bond stress at early age of concrete. They provided an empirical equation for the pullout specimens. This was conservative for matured concrete specimens and did not specify the mode of failure, pull-out and splitting failure.

$$\tau_u = 0.083035\sqrt{f_c'}\left(3.5 + 3.4\frac{C}{d_b} + 57\frac{d_b}{l_e}\right) \quad (2.18)$$

Aslani, F. and Nejadi, S. (2012) [39] forwarded an empirical formula, which is derived from the self-compacting concrete specimens.

$$\tau_u = f_c'^{0.55}\left(0.672\left(\frac{C}{d_b}\right)^{0.6} + 4.8\frac{d_b}{l_e}\right) \quad (2.19)$$

Table 2.1. Summarized of Bond Strength Equations in different Codes and Empirical Equations

No	Codes and predicted models	Empirical equations for bond stress (MPa)	Remark
1	ESEN 1992 1	$f_{bd} = 2.25\eta_1\eta_2 f_{ctd}$	-
2	(ACI) 318 odes	$\tau = \frac{f_y A_b}{\pi d_b l_b}$	It was good by considering the type of concrete
3	CEB-FIP Model Code	$\tau_u = 2.5\ \sqrt{f_c'}$	Only considered pullout bond failure mode and concrete strength as a parameter
4	Huang et al. model code	$\tau_u = 0.45 f_c'$	Only considered concrete strength as the parameter
5	Orangun et al.	$\tau_u = 0.083035\sqrt{f_c'}\left(1.2 + 3\frac{C}{d_b} + 50\frac{d_b}{l_d}\right)$	-
6	Darwin et al.	$\tau_u = 0.083035\sqrt{f_c'}\left(6.67\left(0.5 + \frac{C_{min}}{d_b}\right)\left(0.92 + 0.08\frac{C_{max}}{C_{min}}\right) + 235.62\frac{d_b}{l_d}\right)$	-
7	Shima(1987)	$\tau = 0.9\ f_c'^{\frac{2}{3}}\left(1 - e^{-40\left(\frac{s}{d_b}\right)^{0.6}}\right)$	Only considered long embedment length
8	Champman and Shah (1987)	$\tau_u = 0.083035\sqrt{f_c'}\left(3.5 + 3.4\frac{C}{d_b} + 57\frac{d_b}{l_e}\right)$	Not considered Mode of bond failures
9	Aslani and Nejadi (2012)	$\tau_u = f_c'^{0.55}\left(0.672\left(\frac{C}{d_b}\right)^{0.6} + 4.8\frac{d_b}{l_e}\right)$	Not distinguish the bond strength failure modes

3. MATERIAL AND METHODS

3.1 Introduction

This portion describes the experimental programs followed throughout sample preparation, experimental work, and test setup. The experimental work and testing setup were carried out in the Addis Ababa Institute of Technology's (AAiT) construction material laboratory. The research was started by replacing the coarse aggregate with steel slag aggregate within 25% increments.

3.2 Material properties

The materials used for this study includes cement, fine aggregate, natural coarse aggregate, steel slag aggregate, water and reinforcement bar.

3.2.1 Cement

This study was used the Ordinary Portland Cement (OPC) from the local market. Type-1 Dangote Ordinary Portland Cement is used in this research which has a grade 42.5R and its specific gravity is 3.15.

3.2.2 Aggregate

Aggregate comprises coarse and fine aggregate, which covers 65-75 percent of the volume of concrete. For this study, the aggregate was taken from the same source, to eradicate any property variances. To ensure that the materials meet the specifications for concrete work, all necessary laboratory tests were done, including bulk specific gravity and water observation, moisture content, unit weight, sieve analysis of aggregate, and etc., according to Abebe Dinku Construction Material Laboratory Manual [40]. Before the properties of aggregate were assessed, the aggregate was washed to eliminate impurities like organic debris, and any other dust particles. After drying, the aggregate was placed in a plastic bag to keep the moisture level consistent until mixing time.

3.2.2.1 Fine Aggregate

Fine aggregates used in concrete are passing through a 9.5 mm sieve and almost completely passing with 4.75 mm sieve but predominantly retained on a 0.075 mm sieve according to ASTM C-125 [41]. The fine aggregate used for this investigation was natural sand obtained from the Werabe Sand supplier, and it is used after sieved with a 4.75 mm sieve.

Table 3.1. Physical property of fine aggregate

No	Physical property tests	Test results
1	Bulk density	1490.97 kg/m^3
2	Moisture content	4.65%
3	Silt content	1.33%
4	Water absorption capacity	2.27%
5	Bulk specific gravity	2.45 g/cm^3
6	Finesse modulus	2.71

Table 3.2. Fine aggregate particle size distribution

Sieve size (mm)	Weight retained (g)	Percent of retained	Percent of cumulative retained	Percent of cumulative passing	ASTM C 33 [42] percent of passing
9.5	0	0	0	100	100
4.75	0.6	0.12	0.12	99.88	95-100
2.36	21.9	4.38	4.5	95.5	80-100
1.18	69.8	13.96	18.46	81.54	50-85
0.6	177.8	35.56	54.02	45.98	25-60
0.3	201.9	40.38	94.4	5.6	5-30
0.15	25.9	5.18	99.58	0.42	0-10
Pan	2.1	0.42	100	0	0

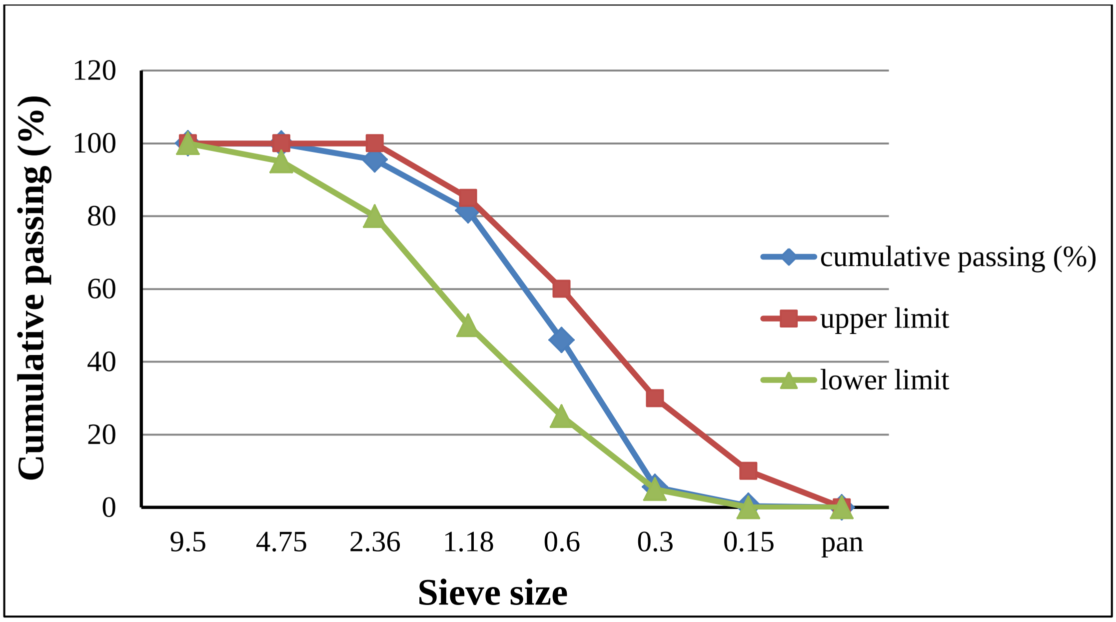

Figure 3.1. Particle size distribution curve for fine aggregate

3.2.2.2 Coarse Aggregate

According to ASTM C-125 standard, coarse aggregates are predominantly retained on 4.75mm sieve size. For this study, a basaltic crushed rock coarse aggregates were used which is taken from local material supplier. The coarse aggregates that used for this research have a nominal aggregate size in between 4.75 mm – 25 mm according to ASTM C 33 [42]. The physical Properties of coarse aggregates were done as shown on Table 3.3.

Table 3.3. Physical property of coarse aggregate

No	Physical property tests	Test results
1	Bulk density	1570.71kg/m^3
2	Moisture content	1.28%
3	Impact value	6.5%
4	Water absorption capacity	1.27%
5	Bulk Specific gravity	2.68g/cm^3
6	Finesse modulus	6.99

Table 3.4. Coarse aggregate particle size distribution

Sieve size (mm)	Weight retained (g)	Percent of retained	Percent of cumulative retained	Percent of cumulative passing	ASTM C 33 percent of passing
25	0	0	0	100	95-100
19	231.2	11.56	11.56	88.44	-
12.5	882	44.1	55.66	44.34	25-60
9.5	636.2	31.81	87.47	12.53	-
4.75	247	12.35	99.82	0.18	0-10
Pan	3.6	0.18	100	0	0

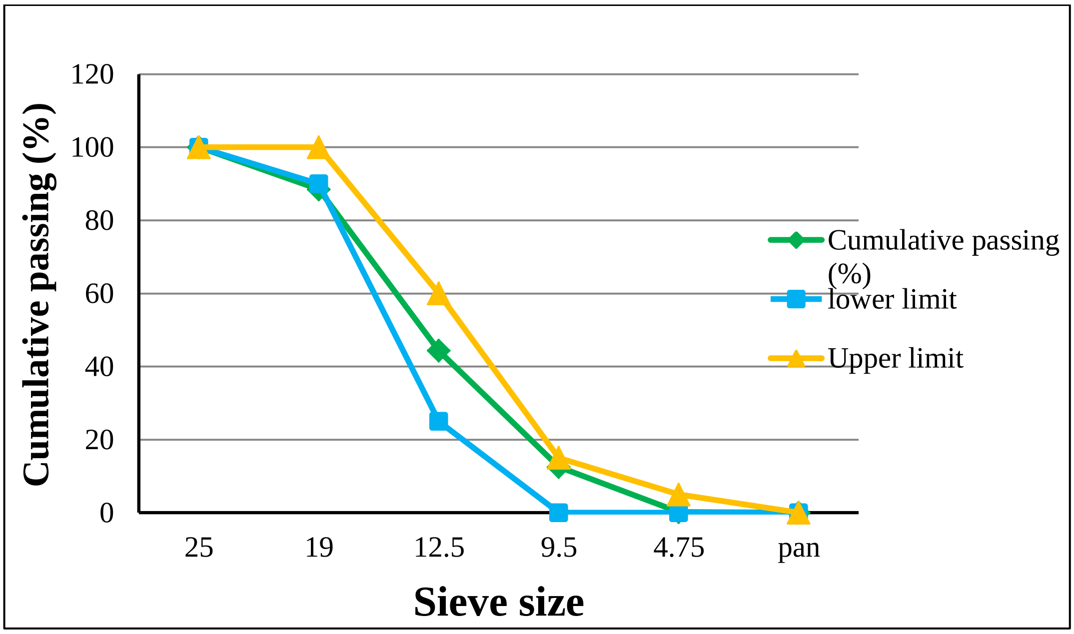

Figure 3.2. Particle size distribution curve for coarse aggregate

3.2.2.3 Steel Slag Aggregate

Steel slag aggregate used for this experimental investigation was obtained from Kalti Metal Production Industry. It was cooled with air and it was subjected to screening, manually crushed and sieving to prepare for concrete mix. In addition, a pretreatment was carried out by exposing the slag to outdoor weather for rain and sunlight for at least three month. The SSA used for this study has a nominal aggregate size of in between 4.75 mm - 25 mm according to ASTM C 33 [42]. On the other way the chemical composition of steel slag is typically stated by in terms of main oxides and minor oxides.

Physical property and chemical composition of steel slag are studied as given in Table 3.5 and Table 3.6 respectively.

Figure 3.3. Steel Slag Aggregate

Table 3.5. Physical property of steel slag aggregate

No	Physical property tests	Test results
1	Bulk density	1368.57kg/m^3
2	Moisture content	1.04%
3	Impact value	16.3%
4	Water absorption capacity	2.15%
5	Bulk Specific gravity	2.35g/cm^3
6	Finesse modulus	6.98

Table 3.6. Chemical composition of steel slag aggregate

Oxides	SiO_2	Al_2O	Fe_2O_3	CaO	MgO	Na_2O	K_2O	MnO	P_2O_5	TiO_2	H_2O	LOI
Composition (%)	55.62	14.18	10.94	1.36	1.08	0.56	3.44	11.26	0.07	0.54	0.26	<0.01

Table 3.7. Steel slag aggregate particle size distribution

Sieve size (mm)	Weight Retained (g)	Percent of retained	Percent of cumulative retained	Percent of cumulative passing	ASTM C 33 percent of passing
25	0	0	0	100	95-100
19	293.7	14.69	14.69	85.31	-
12.5	981.8	49.09	63.78	36.22	25-60
9.5	414.6	20.73	84.51	15.49	-
4.75	292.3	14.62	99.13	0.87	0-10
pan	17.6	0.87	100	0	0

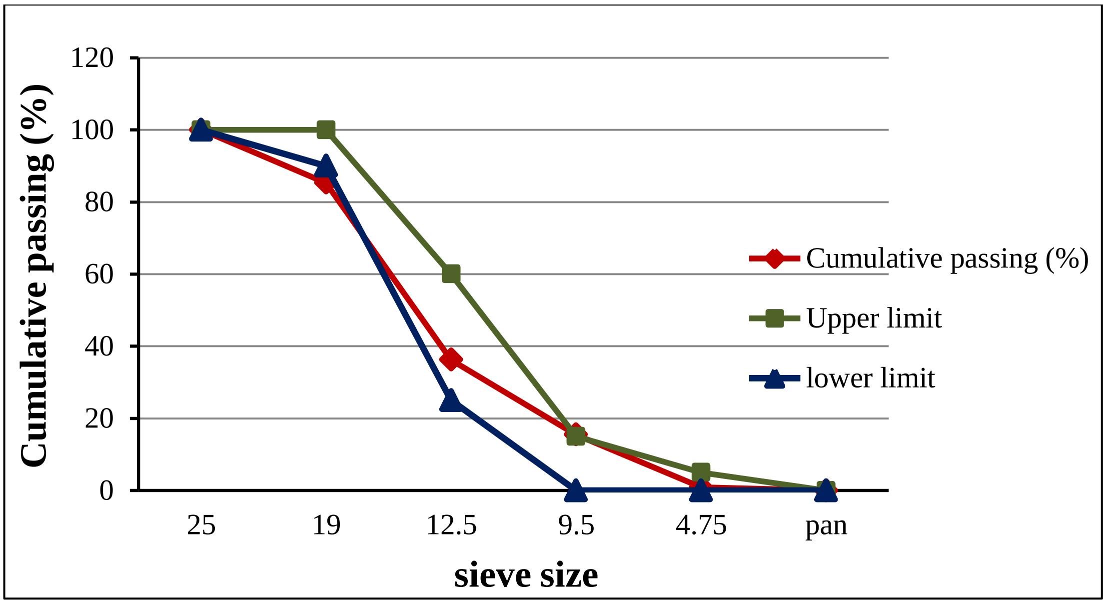

Figure 3.4. Particle size distribution curve for steel slag aggregate

3.2.3 Water

Water is also an essential ingredient of concrete since it plays a strong contribution to form hydration with cement. In addition, it used as to wash materials, to mix concrete and also to cure concrete specimens. So, water must be clean and potable means didn’t contain impurities and dusts. The water used in this investigation is from AAiT construction material laboratory water supply pipe, which is tap water.

3.2.4 Reinforcement Bar

The normal strength deformed reinforcement bars were used for all test specimens, which is Turkey produced type. The nominal diameter of the bar used for this study was 12, 14 and 16 mm. To determine the mechanical properties of the reinforcement bar, uniaxial tensile test was conducted by using Universal test machine as shown in Figure 3.5 in construction material laboratory of Addis Ababa institute of Technology. The mechanical properties of the steel bars are provided in Table 3.8.

Figure 3.5. Universal Testing Machine

Table 3.8. Mechanical properties of the reinforcement bars

Diameter	Average diameter (mm)	Average Yield load (KN)	Average Failure load (KN)	Average Yield strength (MPa)	Average Failure strength (MPa)	Average Elongation (%)
Φ12	12.05	74.7	86.1	654.38	755.40	23.13
Φ14	14.12	87.5	105.3	559.07	672.81	22.90
Φ16	16.07	117.8	142.05	581.29	701.04	22.95

3.3 Concrete Mix Design

According to literatures, the bond strength closely associated to the mixing procedure of concrete as well as its strength. The targeted 28-day compressive strength was C-30 representing medium or normal grade of concrete. The mix design was done by using ACI 211.1-91 [43] standard procedure and specification. And also the replacement of coarse aggregate by SSA was done by volume. The detailed mix design calculation is attached in appendix B. The quantity of each ingredient of concrete is given in Table 3.9.

Table 3.9. Quantity of materials required for unit volume concrete

Percentage of steel slag (%)	Cement (kg/m^3)	Fine aggregate (kg/m^3)	Coarse aggregate (kg/m^3)		Adjusted free Water (kg/m^3)
			NA	SSA	
0	406.82	717.90	1068.08	0	161.81
25	406.82	717.90	801.06	234.41	164.44
50	406.82	717.90	534.04	468.83	167.06
75	406.82	717.90	267.02	703.24	169.69
100	406.82	717.90	0	937.65	172.32

Natural aggregate (NA), steel slag aggregate (SSA)

Table 3.10. Concrete mixes description

No	Mix ID	Description
1	(SSA-0)	Concrete mixes with 0% steel slag aggregate
2	(SSA-25)	Concrete mixes with 25% of natural coarse aggregate replaced by steel slag aggregate
3	(SSA-50)	Concrete mixes with 50% of natural coarse aggregate replaced by steel slag aggregate
4	(SSA-75)	Concrete mixes with 75% of natural coarse aggregate replaced by steel slag aggregate
5	(SSA-100)	Concrete mixes containing 100% of SSA as natural coarse aggregate

3.4 Test Specimen

In this paper, the specimens were selected based on the replacement percentage of SSA. The pullout tests were used to study the bond behavior of steel bar with recycled concrete member considering as the parameter of replacement percentage of steel slag as coarse aggregate and reinforcement bar diameter. The pullout specimens were casted form 5 different concrete mixes with deformed steel bar diameter of (12, 14, 16 mm). Workability was measured for each fresh concrete at the time of mixing. And also on hardened concrete, compressive strength, splitting tensile strength, and bond strength were tested. The total number of the specimens, 30 cube (with 150 mm side size) and 30 cylinder with a diameter of 150 mm × 300 mm in height for compressive strength and splitting tensile strength of concrete respectively, and for pullout bond test 45 specimens of cylinder with a diameter of 150 mm × 300 mm in height has been casted. Each group had three identical specimens. The details of the specimen parameter were listed on Table 3.11 below.

Table 3.11. Tests specimen description and number of specimens

Mix ID (Specimens)	**Pull-out test parameters**				**Pullout test**	**Compressive strength test**		**Splitting tensile strength test**	
	Diameter of bar (mm)	L_e (mm)	L_u(loaded end + free end) (mm)	Cover (mm)	28 day	7 day	28 day	7 day	28 day
SSA-0	12	60	240	69	3	3	3	3	3
	14	70	230	68	3				
	16	80	220	67	3				
SSA-25	12	60	240	69	3	3	3	3	3
	14	70	230	68	3				
	16	80	220	67	3				
SSA-50	12	60	240	69	3	3	3	3	3
	14	70	230	68	3				
	16	80	220	67	3				
SSA-75	12	60	240	69	3	3	3	3	3
	14	70	230	68	3				
	16	80	220	67	3				
SSA-100	12	60	240	69	3	3	3	3	3
	14	70	230	68	3				
	16	80	220	67	3				
Total number of test specimens					45	30		30	

Embedment length (L_e), unbound length (L_u)

3.5 Specimen Preparation

The pull-out specimens were cylindrical with a diameter of 150 mm × 300 mm in height, and a single bar was anchored vertically along the central axis of concrete specimen and it was prepared from five different concrete mixes and three bar diameters.

Figure 3.6. Painting of Machine grease on External surface of PVC tube

3.5.1 Pull-out test Specimen's geometry

The pull-out test specimens were a concrete cylinder with 150 mm diameter and 300 mm height with centrally fixed 12 mm, 14 mm and 16 mm deformed bar with length 1000 mm. Free end of the rebar was projected through the center holed steel plate about 80 mm to measure the free end slip for each diameter of bar. While the loaded end was extended about 620 mm in order to grip the rebar by applying the tensile force for pullout test and also end slip was measured by transducers at the free end. The bond length of the pullout specimens was five times bar diameter (i.e., $L_e = 5d_b$) as suggested by RILEM [33]. This short embedment length is allowed a uniform bond stress distribution with the representative slippage recorded. To achieve the required bonded length at the center of the specimen, PVC tubes were used to protect the rebar from bonding with the concrete at loaded and free end. The PVC tube must be smooth and neither restrains the slippage of the bar nor affects the transfer of force between the bar and concrete. The end of PVC tube was surrounded by plastic tape to prevent the entrance of concrete into it moreover to increase the surface smoothness of the PVC tube it was smeared with machine grease as shown in Figure 3.6.

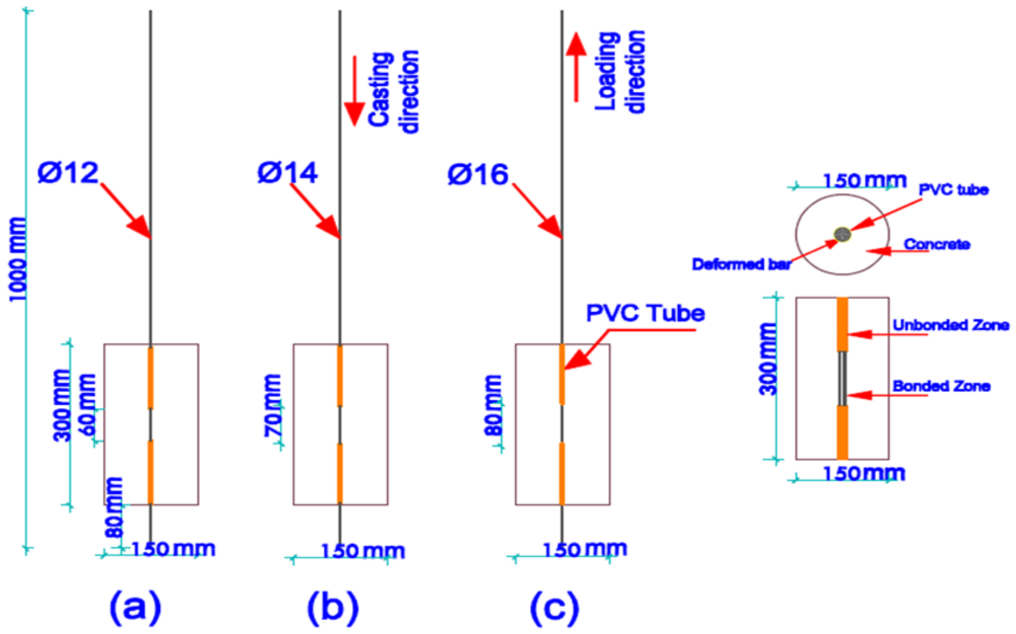

Figure 3.7. Pullout specimen's geometry

3.6 Concretes mix

The concrete was mixed in laboratory with electrically powered mixer machine as shown on Figure 3.8. Making and curing of test specimens were conducted according to ASTM C-192 [44]. In the mixer, the coarse aggregate was added first, then the cement, and finally the fine aggregate, and it was mixed without the addition of water. The mixing was continued by adding water in wet condition until the concrete achieved uniform consistency.

Figure 3.8. Concrete mixing

As soon as the mixing was finished the workability of the concrete was checked by slump test. The Slump test of every fresh concrete is measured according to ASTM C-143 [45]. The fresh concrete was added to the slump cone with in three layer of compaction to check the workability of the concrete.

Figure 3.9. Slump measurement

Casting of the specimen into the prepared cube and cylinder molds was followed after checking the workability of concrete. Before casting, the inner part of molds is smeared with machine oil. For the pullout test specimens the bar was fixed vertical and projected about 80 mm to the bottom part of cylinder through center holed steel plate. The center alignment of the bar was keep with mechanical prepared thin steel bar. Finally, the fresh concrete was poured in to the papered mold and compacted with Internal Vibrator under controlled vibration. After fully vibrating, the mold was filled with the concrete and vibrated again to ensure the well-consolidated concrete. After a period of 24 hrs the specimens removed from the mold and placed in water tank for curing till test days as shown in Figure 3.13.

Figure 3.10. Oil smeared molds

Figure 3.11. Casting and vibration of concrete

Figure 3.12. Concrete Specimens after casting

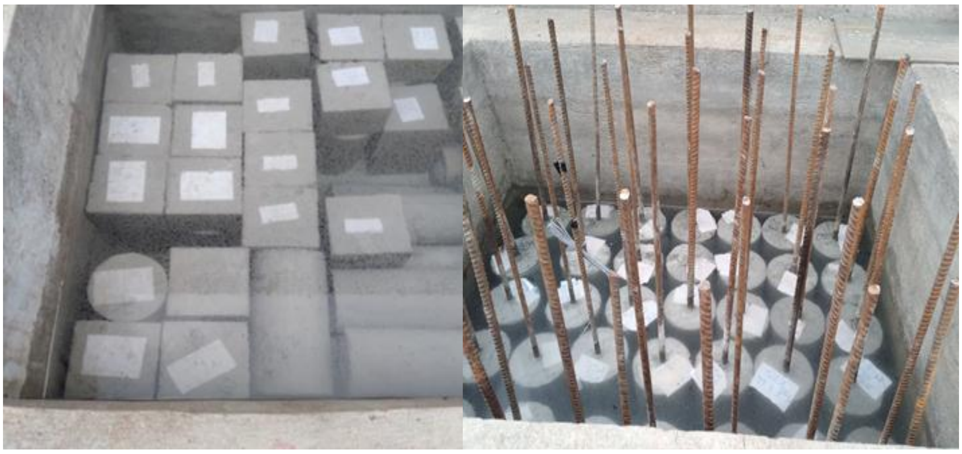

Figure 3.13. Curing of concrete specimens

3.7 Experimental set-up and testing

Compressive Strength Test

The compressive strength test was done with cubes with the size of 150×150×150 mm. After the specimens were removed from the curing tank the test was conducted in moist condition followed form the concrete surface dried with absorbent cloth. The test was done according to ASTM C-39 [46]. Compressive strength of the concrete was measured for seven and twenty-eight days curing by using Universal Test Machine as shown on Figure 3.14. The rate of loading of the machine is 0.28 MPa/sec and its load capacity is 3000 kN. Three cubes of each concrete mixes were tested for concrete compressive strength.

Figure 3.14. Test setup of Compressive strength test

Splitting Tensile Strength Test

Splitting tensile strength test was doing using indirect tensile test method of measurement. In this approach, a diametric compressive force is applied along the length of a cylindrical concrete specimen with placing the plywood strips at the lower and upper center with a constant rate of range (689 to 1380 kPa/min) up to failure happens ASTM C-496-96 [47]. Three cylindrical specimens of each concrete mixes were tested at 7^{th} day and 28^{th} day for splitting tensile strength of concrete.

Figure 3.15. Test setup of Splitting tensile strength test

The splitting tensile strength of concrete is determined by the equation

$$f_{ct} = \frac{2P}{\pi d_b l_b} \quad (3.1)$$

Where

P is the failure load

d_b is the cylinder diameter

l_b is the length of the cylinder

Pull-out Bond Strength Test

Pullout is one of the methods that measure the bond strength between the concrete and reinforcement bar. For this study, pullout test method is used to determine the bond strength of specimens, and it was conducted at 28^{th} day. The bond strength test instrument was mainly designed to measure the bond tensile load and the slip of the specimens. Center-Hole Jack was used for pullout bond test and the extended reinforced bar passed through the Center-Hole Jack and it was grasped by Bolts, it was installed on the upper end of the machine which has different diameter size. The load was applied by using the Center-Hole Jack pullout testing machine which has a capacity of 130 kN and the applied load was recorded by Center-Hole Load Cell as shown below in Figure 3.17. Further, the free end slip of reinforcing bar was measured by Transducer during the testing going on. The Load cell and Transducer were connected with Data logger, to display the recorded applied load and end slip on its screen. The experimental results were saved with the USB flash disk through Data logger.

Figure 3.16. Specimens prepared for pullout test

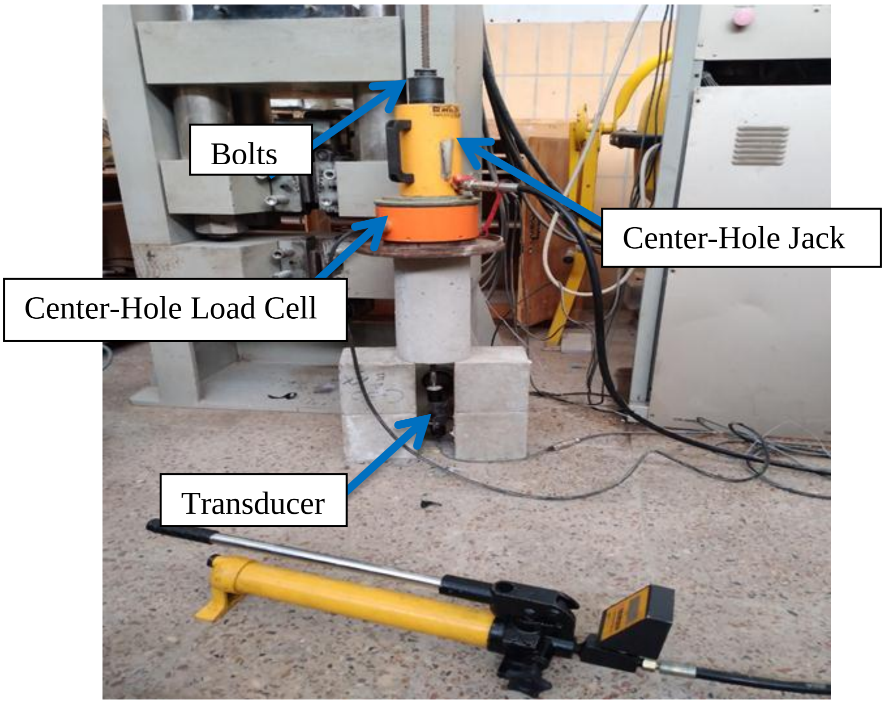

Figure 3.17. Pull-out test setup

Figure 3.18. Data logger

4. RESULT AND DISCUSSION

The summary of all experimental test results were discussed on this chapter that would be presented like the outcome of the experimental program on the mechanical property of the concrete and also the bond behavior of reinforced concrete member. The test result of pull-out bond strength test was the tensile force and slip which is an input to represent the bond stress to slip relation. Those results were discussed by using the table, bar graph and line graph.

4.1 Fresh Concrete Properties

4.1.1 Slump test

Slump test is conducted on fresh concrete to check the workability and consistence of concrete. On this study, Slump tests were performed for each concrete mixes. The results of slump test shown that as the percentage of SSA replacement increased from 0% to 100% at 25% of interval the slump value shown decrement with in the medium degree of workability. Due to water absorption capacity of steel slag is greater than natural aggregate, and steel slag aggregate has rough surface and irregular shape, workability of the concrete was decreased. The requirement of water increased as the aggregate become more angular and rough textured [43]. Workability of concrete decreases as the steel slag percentage of replacement increases [13]. The slump values for all concrete mixes were presented on Figure 4.1 below.

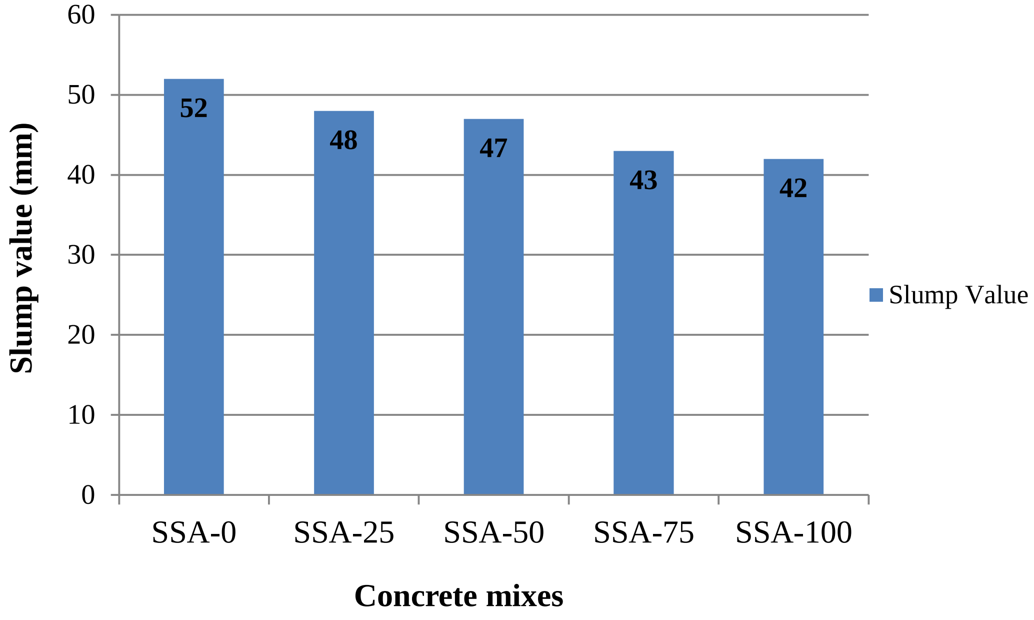

Figure 4.1. Slump values of concrete mixes

4.2 Hardened Concrete Properties

One of the hardened properties of concrete is its mechanical property, which comprises compressive strength and splitting tensile strength. For the C-30 grade of concrete containing steel slag aggregate, compressive strength and splitting tensile strength tests were performed for 7th and 28th days.

4.2.1 Compressive Strength of Concrete

The results of concrete's compressive strength tests were discussed further below. The average test results of compressive strength of the concrete with steel slag aggregate replacement are shown on Table 4.1. The detailed results are provided in Appendix D.

Table 4.1. Average compressive strength of concrete

No	Specimens	Average cubical compressive strength (MPa)	
		7th day	28th day
1	SSA-0	31.12	43.46
2	SSA-25	33.26	45.68
3	SSA-50	34.27	47.98
4	SSA-75	31.25	43.24
5	SSA-100	26.97	39.13

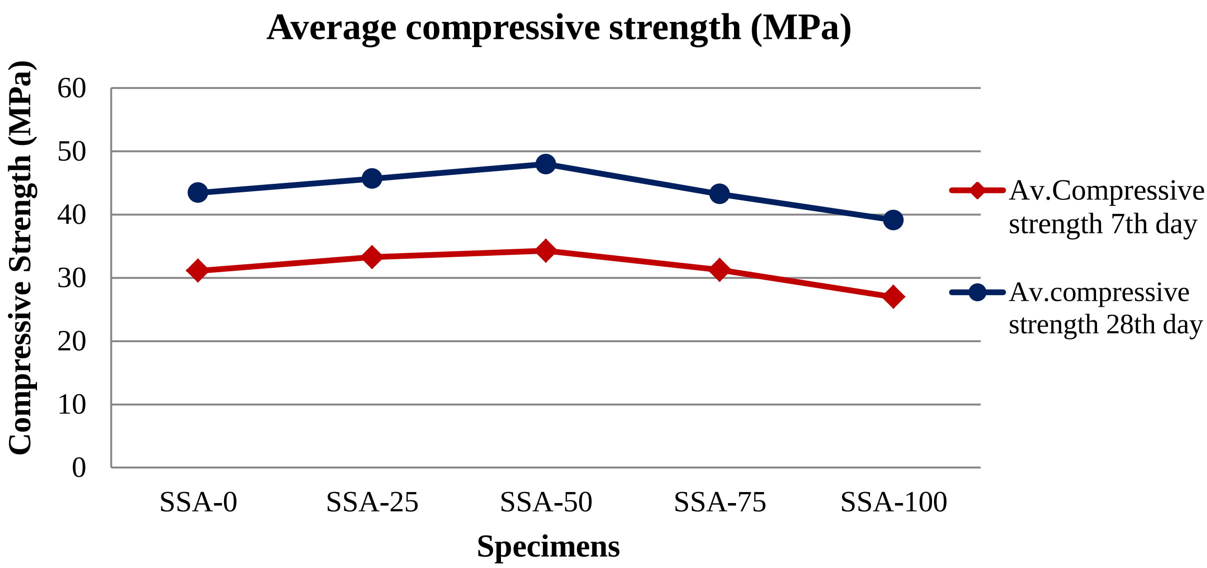

Figure 4.2. Average compressive strength of concrete specimens

From Figure 4.2, it can be observed that the compressive strength of the concrete increased up to 50% replacement of coarse aggregate with steel slag, beyond which the compressive strength decreased on further replacement. As it can be observed that the 28^{th} day compressive strength, SSA-50 increased by 10.40% and SSA-100 decreased by 9.96% as compared to the control specimens. It indicates that the optimum replacement is 50%. Steel slag aggregate has rough surface and angular shape; the shape and surface roughness play an important role in improving the concrete strength by allowing the aggregate and cement paste to better interlock.

4.2.2 Splitting Tensile Strength of Concrete

The splitting tensile test consists of applying a compressive line load along the concrete cylinder's opposite side, with its axis horizontally between the patterns. Due to this tension, the specimen fails along the loaded diameter. The splitting tensile strength test results presented on Figure 4.3 as shown below. The detailed splitting tensile test results are given in Appendix E.

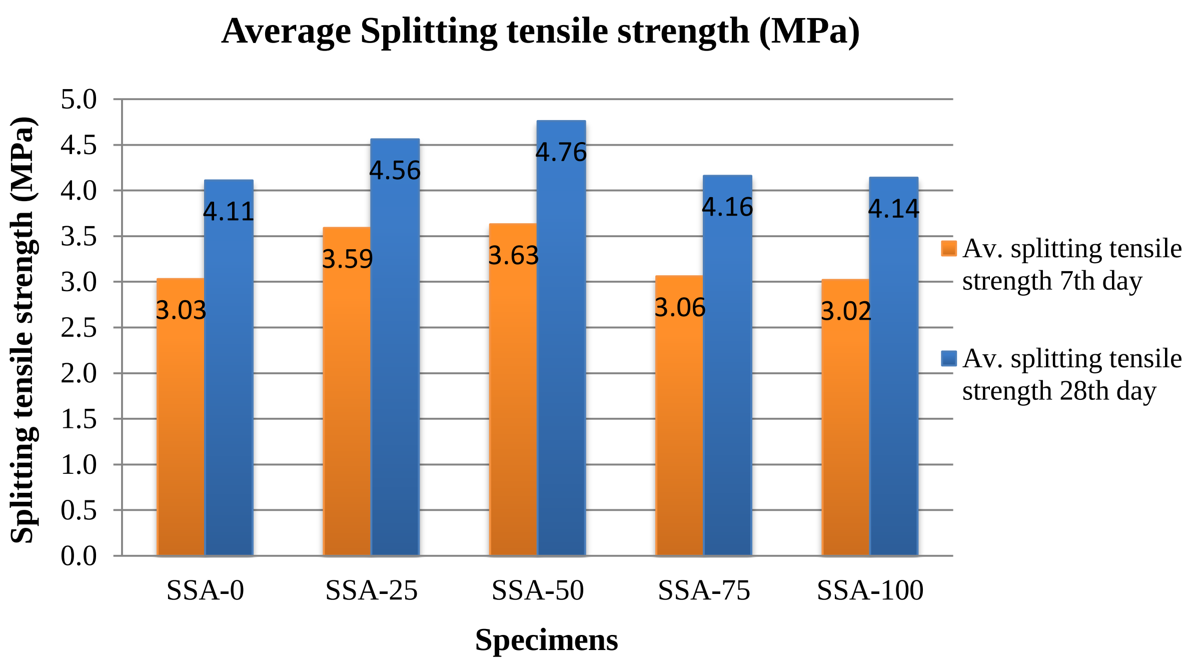

Figure 4.3. Average Splitting tensile strength of concrete specimens

The result shown that the splitting tensile strength of steel slag aggregate concrete is greater than the conventional concrete. It describe that steel slag aggregate has higher tensile strength than natural aggregate. Likewise the compressive strength, splittng tensile strength is also maximum at 50% replacment of SSA as shown on Figure 4.3. It indicates that the optimum replacement is 50% which increases the splitting tensile strength of 28th day by 15.82%. It describes that steel slag aggregate have more ductile property than the conventional aggregate.

4.3 Bond Strength

Bond stress is the shear stress around the embedded length of the reinforced bar and the concrete, and for short embedment length the bond stress is usually considered as uniform.

The bond strength is determined by dividing the pullout load to the reinforced bar's embedding area. The bond strength (τ) is given by

$$\tau = \frac{P}{\pi d_b l_e} \quad (4.1)$$

where

P is the pullout tensile load

d_b is the diameter of the bar

l_e is the embedment length

And also the Normalized ultimate bond strength calculated by

$$\tau_u^* = \frac{\tau_u}{\sqrt{f_c'}} \qquad (4.2)$$

Where

τ_u is the ultimate bond stress

f_c' is cylindrical compressive strength of the concrete

Table 4.2. Pullout Test Results

No	Specimen	Diameter of Bar (mm)	Average Failure Load (kN)	Average ultimate Bond Strength (MPa)	Normalized Bond Strength	Average Slip (mm)	Mode of Failure
1	SSA-0	12	41.83	18.49	3.14	0.98	Pullout
		14	51.27	16.65	2.82	1.16	Pullout
		16	66.33	16.50	2.8	0.39	Splitting
2	SSA-25	12	45.43	20.09	3.32	0.95	Pullout
		14	51.6	16.76	2.77	1.12	Pullout
		16	71.17	17.70	2.93	0.65	Splitting
3	SSA-50	12	43.1	19.05	3.08	0.88	Pullout
		14	56.97	18.50	2.99	1.05	Pullout
		16	71.33	17.74	2.86	0.51	Splitting
4	SSA-75	12	38.57	17.05	2.9	0.96	Pullout
		14	51.73	16.8	2.86	1.56	Pullout
		16	65.8	16.36	2.78	0.57	Splitting
5	SSA-100	12	37.35	16.51	2.95	1.32	Pullout
		14	49.07	15.94	2.85	1.55	Pullout
		16	63.2	15.72	2.81	0.49	Splitting

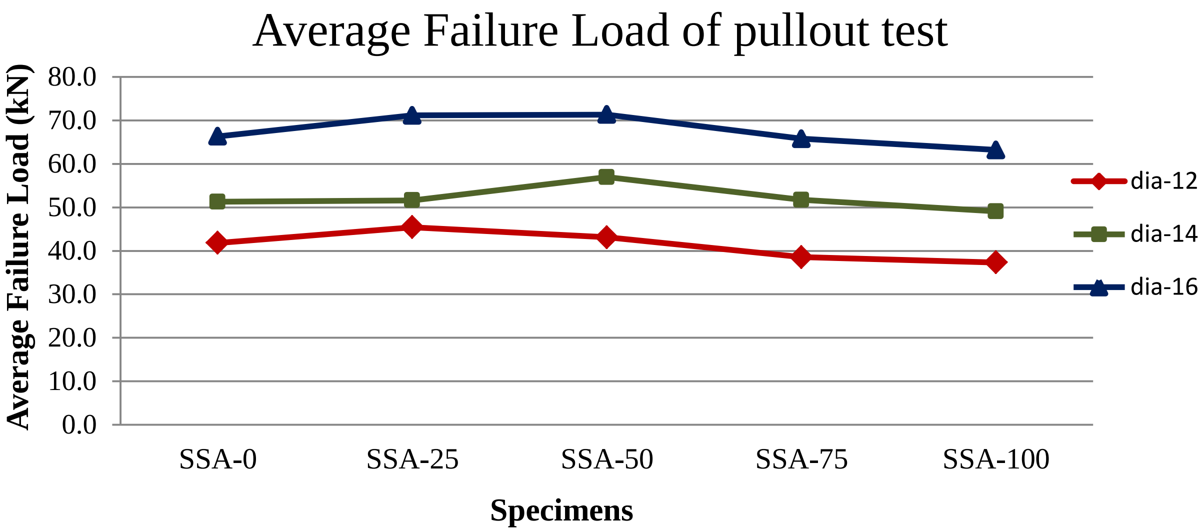

Figure 4.4. Average Failure Loads of pullout test

Form the above Table 4.2 it observed that SSA-50 yields the maximum bond failure load than the control concrete specimen (SSA-0) and also SSA-100 has the compatible average failure load with conventional concrete specimen. For diameters of bar 12, 14, and 16 mm, the pullout failure load of SSA-50 specimens was increased by 3.04%, 11.12%, and 7.54%, respectively. Furthermore, for diameters of bar 12, 14, and 16 mm, the bond failure load of SSA-100 has decreased by 10.71%, 4.29%, and 4.72 %, respectively, when compared to SSA-0.

On the other hand bar diameter size also affects the bond failure load, the larger bar diameter have larger bond length so required maximum forces to cause either a splitting or pullout failure. From Figure 4.4 it presented that the average pullout failure load of 16 mm bar diameter was greater than 12 mm, and 14 mm for all specimens. The detailed pullout test results are obtained in Appendix F.

4.3.1 Ultimate Bond Stress

Pullout tests were carried out on specimens with different steel slag aggregate replacements as coarse aggregate and rebar diameter (12 mm, 14 mm and 16 mm). For a total of 45 specimens, pullout tests were performed at the age of 28 days. After recording the failure load from the pullout test, the ultimate bond strength was determined. The experimental result of average ultimate bond strength was presented for each replacement of steel slag aggregate and bar diameter on Figure 4.5 below.

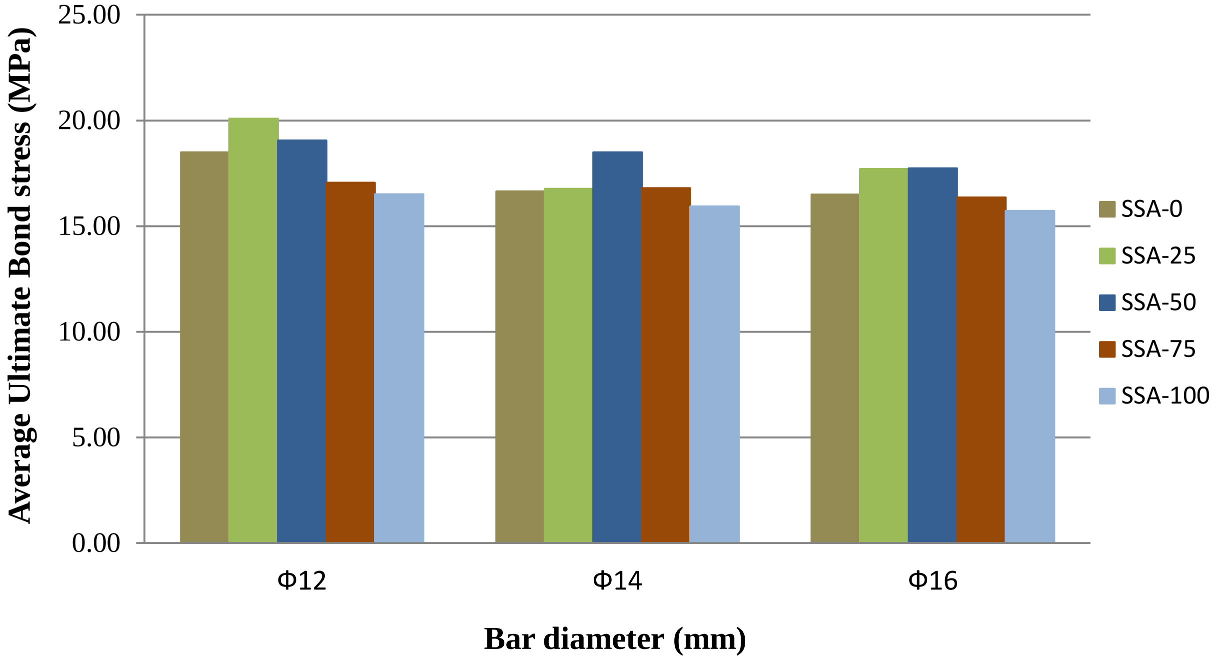

Figure 4.5. Ultimate bond stress values of pullout test

Effect of Steel Slag Aggregate on the Ultimate Bond Strength

Almost for all pullout tests the ultimate bond strength was a maximum on the specimen SSA-50 as a shown on Figure 4.5. It observed that the ultimate bond strength of SSA-50 increased by 3.04%, 11.12%, and 7.54% for 12, 14, and 16mm bar diameter, respectively. As discussed before compressive and splitting tensile strength of SSA-50 concrete specimen was greater than the control specimen. However, for bond strength, tensile strength of concrete contributes more than compressive strength, and steel slag aggregate performed better in splitting strength. Findings obtained in this study can be supported by Tang, C.W. and Cheng, C.K [48] stated that as the general the bond strength is directly related to compressive and splitting tensile strength of the concrete. When the concrete compressive and splitting strength increased the bond performance between the concrete and rebar also increased and developed higher bond stress before the occurrence of failure.

Effect of Bar Diameter on the Ultimate Bond Strength

The average ultimate bond strength of Φ12, Φ14 and Φ16 deformed steel bars under the smaller embedded length of 5 times diameter of bar 60, 70, and 80 mm, respectively was presented on Table 4.2. From pullout test results, it indicates that the ultimate bond strength of larger bar diameter (16 mm) was smaller than smaller bar diameter (12 mm). Due to the availability of large concrete cover (69 mm) provided for 12 mm bar diameter the bond stress was high. While the concrete cover thickness of 16 mm bar diameter (67 mm) was inadequate to gain the representative bond stress which was lesser than $4.5d_b$, the recommended values on the different standards. It indicates that the greater concrete cover could promote the confinement of rebar and also the splitting resistance of concrete.

The pullout test results presented that the ultimate bond stress of 16 mm bar diameter decreased by 10.76% and 6.88% of 12 mm bar diameter for the specimens of SSA-0 and SSA-50, respectively. The Previous studies [48] support the result obtained on this study that the bond strength was decreased as the diameter of the rebar was increased. The larger bar diameter has the smaller relative bond area, so the bond stress was decreased. In addition, the bar rib height has been the considerable influence on bond property of reinforced concrete.

Failure Mode

During the pullout testing, the load was transferred in between the rebar and the concrete with an adhesion, mechanical interlock and friction. The inclined rib of the deformed rebar acted as interlocking bearing with embedded concrete. The rib of steel bar will either split the concrete by pushing it away or crush the concrete by enclosing it in the area between them when the load is transferred between the deformed bar and the concrete.

In general, the failure mode of pullout bond strength test depends on bar diameter, concrete cover, bar rib geometry, and concrete compressive and tensile strength. The bond strength is usually controlled by the splitting strength of the concrete [49]. Pullout failure and splitting concrete failure are the common mode of bond failures. In this study, almost all specimens of 12 mm and 14 mm bar diameter were failed with pullout failure mode as shown Figure 4.6 (a) due to having enough concrete cover thickness (69 mm and 68 mm). When the resistance of the surrounding concrete exceeds the radial force, pullout bond failure will occurred, so the role of confinement is significant.

The concrete cover of 16 mm diameter specimens was smaller than 12 mm and 14 mm under the same embedded length $5d_b$ circumstances, while the bond length was more than 12 mm and 14 mm. Due to the concrete cover thickness for 16 mm diameter of bar is insufficient to resist the radial force generated from loaded rebar the splitting of the concrete cover was exhibited as shown on Figure 4.6 (b). To get the representative bond stress, RILEM [33] standards indicated that the embedded concrete cross sections for pullout test specimens with shorter embedded lengths ($5d_b$) be a minimum of 10 times the bar diameter. When the circumferential tensile resistance created in the concrete was lesser than the radial tensile force of the steel bar, splitting of concrete cover could be produced.

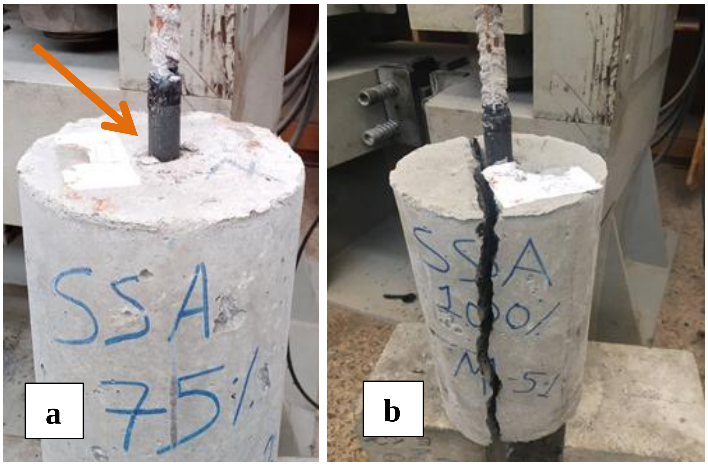

Figure 4.6. Bond strength failure mode: (a) pullout failure, (b) splitting failure

For all concrete specimens failed with splitting, the failure of aggregate was observed on both the conventional aggregate concrete and also steel slag aggregate concrete. There was no the occurrence of cracking on cementations matrix. Due to the surface roughness of steel slag aggregate, the aggregate paste interlock was better on the steel slag aggregate concrete than on the natural aggregate.

4.3.2 Bond Stress – Slip Relationship

In this study, the pullout tensile load and the free end slip was obtained from the experimental pullout test result, and the bond strength was determined by the equation 4.1. Then the bond stress-slip curve can be drawn based on the test results. The bond stress-slip graph for the specimens with different steel slag aggregate replacement and different steel bar diameter are presented on Figure 4.7, 4.8, and 4.9 below.

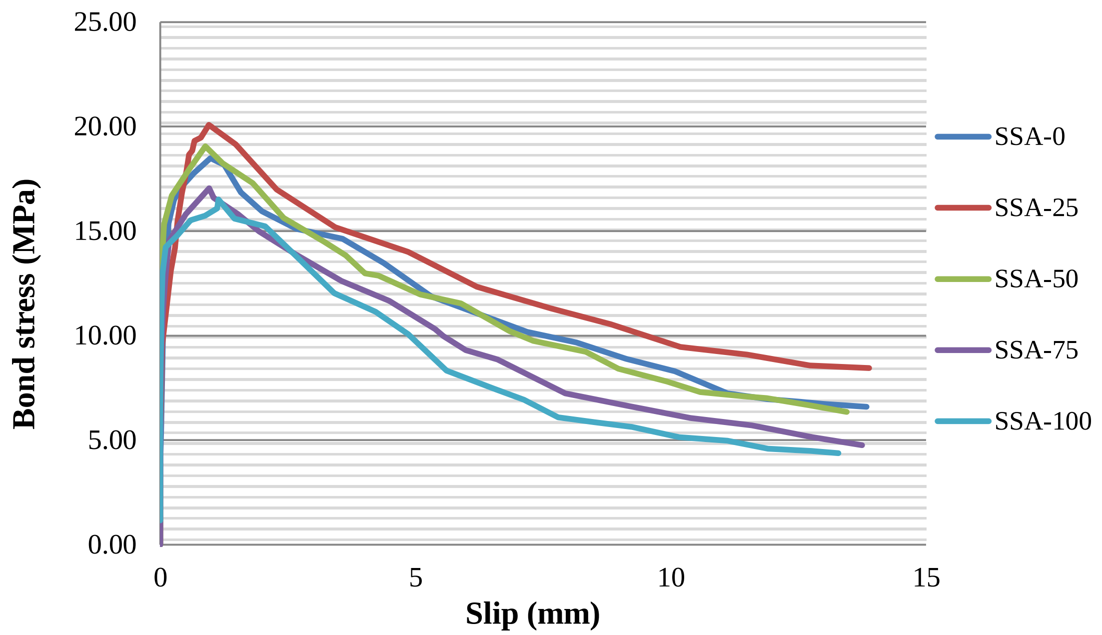

Figure 4.7. Bond stress- Slip curve for specimens with Φ12 rebar

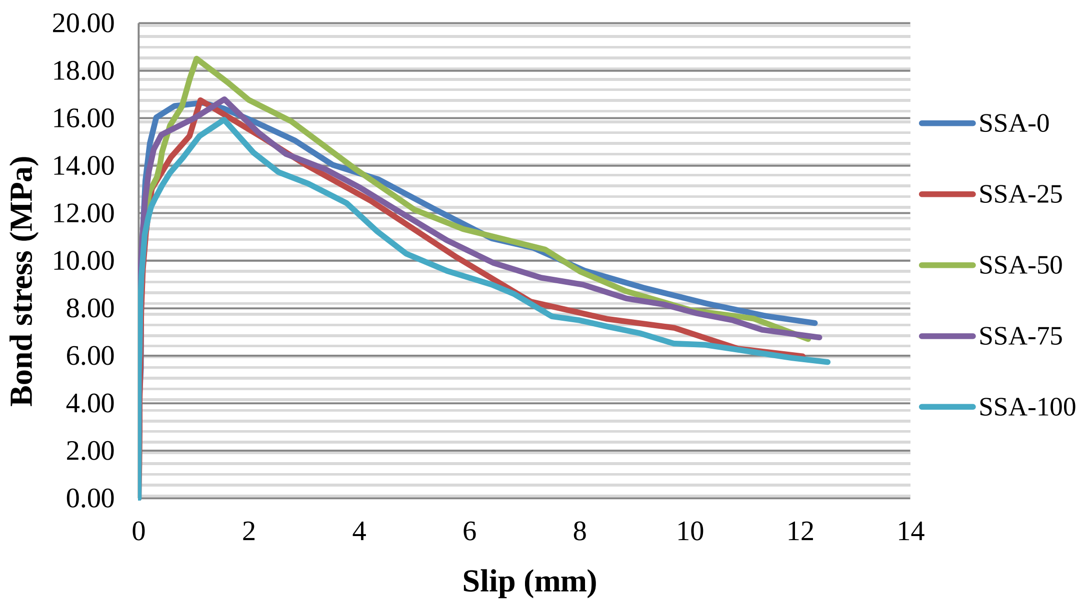

Figure 4. 8. Bond stress- Slip curve for specimens with Φ14 rebar

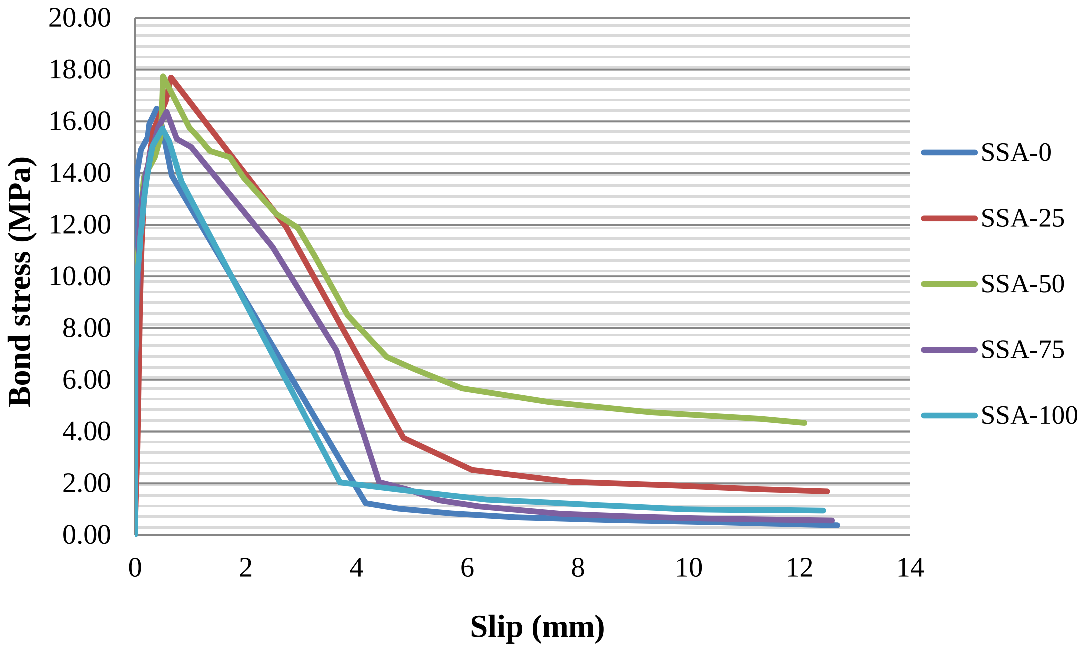

Figure 4.9. Bond stress- Slip curve for specimens with Φ16 rebar

The pullout bond stress-slip curve shows that at the initial stage it was nearly vertical with small slippage for all specimens. It describes that the bond between the concrete and the reinforcement bar is strong so to deboned it needs large pullout tensile load. Followed that the bond stress was rising rapidly and the slip also increased with small value interval. Finally, the bond stress-slip curve declined as the bond stress decreases and the slip increases rapidly. From the result it observed that as the steel slag aggregate replacement increases till 50%, the bond stress also increased, and for further replacement it was decreased.

In general the bond stress-slip curve of the pullout specimen shows that when the bond stress increased steeply at initially, and the slip increased at a small interval. At a time of the bond stress was reached at the maximum value the curve became soften immediately for pullout failure. After attained of the ultimate bond stress the slip was increased and the bond stress was decreased. From the Figure 4.7 and 4.8, it observed that the bond stress-slip curve was almost similar for the specimens with the rebar of 12 mm and 14 mm diameter which are the pullout failure. However, Figure 4.9 showed a radically decrement of bond stress before reaching real ultimate bond stress for the specimens of 16 mm bar diameter, due to splitting of concrete cover. The splitting of concrete cover occurred at smaller slip value. Finally, residual bond stress would be produced by friction between the concrete and the reinforcement bar and slip of rebar significantly increased.

4.4 Predicted Ultimate Bond Strength in different Code Provisions and Empirical Equations

The bond strength between the concrete and steel bar have been studied with different investigators. And the researchers have also investigated the influence of bar diameter, concrete cover, embedment length and traverse confinement on the bond strength. In addition, several researchers have been suggested different empirical equations to calculate the bond strength by considering the factors of bond stress. This study selected some common prediction model codes and empirical equations of bond strength to compare with the test result bond stress. The current code and equations proposed within different literatures did not considered the effect of replacement materials such like SSA on bond strength equation. The comparison of the ultimate bond stresses in between the experimental result and predicted value was provided in Table 4.4 below. Further, this study proposed an empirical equation for ultimate bond strength based on the test results by using MATLAB software regression analysis.

$$\tau_u = 4.31\sqrt{f_c{}'} + 0.95\frac{C}{d_b} - 12.86 \quad (4.3)$$

Table 4.3. Bond strength Parameters

Parameters	SSA-0			SSA-25			SSA-50			SSA-75			SSA-100		
d_b (mm)	12	14	16	12	14	16	12	14	16	12	14	16	12	14	16
L_e (mm)	60	70	80	60	70	80	60	70	80	60	70	80	60	70	80
C (mm)	69	68	67	69	68	67	69	68	67	69	68	67	69	68	67
$f_c{}'$(MPa)	34.77			36.54			38.38			34.59			31.30		
f_{ct} (Mpa)	4.11			4.56			4.76			4.16			4.14		

Table 4.4. Comparison of predicted bond strength with pullout test result

Specimen	Bar Diameter (mm)	$\tau_u$exp (MPa)	τ*exp	Calculated bond strength (MPa)									
				Orangun et al	Darwin et al	Shima	Chapman and Shah	Aslani and Nejadi	ESEN 19921	ACI	CEB-FIP	Huang et al.	Predi. Equ.
SSA -0	12	18.49	3.14	13.93	13.83	9.59	16.87	20.28	4.32	2.98	14.74	15.65	18.02
	14	16.65	2.82	12.62	12.91	9.59	15.38	18.97	4.32	2.98	14.74	15.65	17.17
	16	16.5	2.8	11.63	12.21	9.46	14.27	17.93	4.32	2.98	-	15.65	16.53
SSA -25	12	20.09	3.32	14.28	14.18	9.91	17.29	20.84	4.79	3.05	15.11	16.45	18.66
	14	16.76	2.77	12.94	13.23	9.91	15.77	19.5	4.79	3.05	15.11	16.45	17.81
	16	17.7	2.93	11.93	12.52	9.89	14.63	18.43	4.79	3.05	-	16.45	17.17
SSA -50	12	19.05	3.08	14.64	14.53	10.24	17.72	21.41	5	3.13	15.49	17.27	19.31
	14	18.5	2.99	13.26	13.56	10.24	16.16	20.03	5	3.13	15.49	17.27	18.46
	16	17.74	2.86	12.22	12.83	10.18	14.99	18.94	5	3.13	-	17.27	17.82
SSA -75	12	17.05	2.9	13.89	13.8	9.55	16.82	20.22	4.37	2.97	14.7	15.57	17.95
	14	16.8	2.86	12.59	12.87	9.56	15.34	18.92	4.37	2.97	14.7	15.57	17.1
	16	16.36	2.78	11.6	12.187	9.51	14.23	17.88	4.37	2.97	-	15.57	16.47
SSA -100	12	16.51	2.95	13.227	13.12	8.94	16.01	19.14	4.35	2.82	13.99	14.09	16.72
	14	15.94	2.85	11.97	12.25	8.94	14.59	17.91	4.35	2.82	13.99	14.09	15.87
	16	15.72	2.81	11.04	11.59	8.88	13.54	16.93	4.35	2.82	-	14.09	15.23

Some of the predicted bond strength values were comparative with the experimental results. However, the effect of the steel slag aggregate was not considered with in those investigators predicted equation. But some of the predicted values had a significant difference with the experimental results.

Orangun et al and Darwin et al.

The theoretical bond strength that calculated by using the empirical equations of [36] and [37] shows slight convergence with the test results as shown Table 4.4. When compared to experimental results, the bond stress computed using equations (2.16 and 2.17) is conservative and underestimates the specimen bond strength.

Shima, Chapman and Shah, and Aslani and Nejadi

The estimated equations by Shima [20] yielded underestimate bond strength values for all specimens compare to the experimental results. The influence of bar diameter and concrete compressive strength were also taken into account in this predicted equation.

On the other hand a compatible ultimate bond strength values were obtained from Chapman and Shah [38] empirical equation with the pullout test results. This predicted equation provided underestimated bond strength value for all specimens as shown on Table 4.4. However, the Aslani and Nejadi [39] empirical equation provided the overestimated value of ultimate bond strength for specimens compare to the experimental results. This empirical equation provided non-conservative bond strength values for all specimens.

ESEN 1992 1 and ACI code

The predicted bond strength by using ESEN 1992 1 [34] and ACI code [35] bond strength equations shows significantly lower than the test results. The ESEN 1992 1 code focuses primarily on concrete tensile strength and not considered other factors of bond strength like embedment length and concrete cover thickness and it is proposed for only the conventional concrete. On the other hand the ACI code provision gives more attentions for development length of steel bar in reinforced concrete. The effect of bar diameter and concrete compressive strength on predicted bond strength of specimens with ESEN 1992 1 and ACI codes had no significant effect, while there was a small variation between the specimens with different compressive strength, and the effect of bar diameter was similarly insignificant. For both conventional concrete and steel slag aggregate concrete, the ACI and ESEN codes are more conservative and underestimate the bond strength values of the specimens. ACI code obtained nearly the same bond strength values for all specimens due to the embedment length is very short as compare to the code considered.

CEB-FIP model and Huang et al. model

CEB-FIP model [26] obtained underestimated value for all pullout failed specimens of conventional concrete and steel slag concrete. In addition, Huang et al. [25] prediction model provided a comparative ultimate bond strength values with the experimental results. But as a general it obtained underestimated values of the ultimate bond strength for all specimens. CEB-FIP and Huang et al. prediction model, which is considered the Concrete compressive strength as the only parameter to predict the ultimate bond stress and it does not considered the effect of the other main factors of bond strength and this is the main limitation of those models.

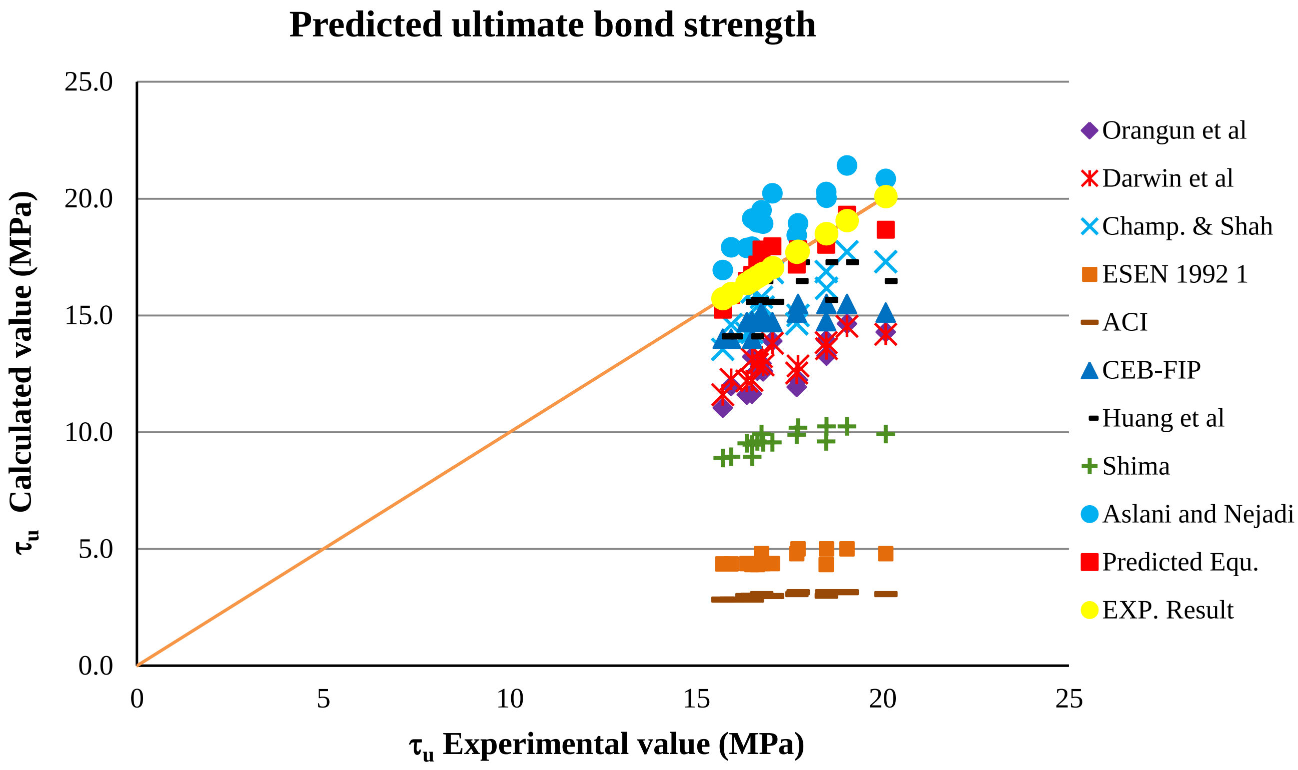

Figure 4.10. Predicted ultimate bond strength for pullout specimens

5. CONCLUTIONS AND RECOMMENDATIONS

5.1 Conclusions

This research investigated the bond behavior of the steel bar embedded with the steel slag aggregate concrete by pullout test. Finally, the following conclusions are drawn from the experimental test results.

1. The workability of concrete decreases as the percentage replacement of steel slag aggregate increases.
2. The compressive and splitting tensile strength of the concrete increases till 50% of the natural coarse aggregate is replaced with steel slag aggregate, while further replacement decreases.
3. The bond strength of specimens' increases up to 50% of the coarse aggregate is replaced by steel slag, after which it decreases.
4. There is no significant difference in bond strength between control concrete specimens and 100% SSA concrete specimens due to the steel slag aggregate concrete has good tensile strength.
5. The experimental bond stress decreases as the bar diameter increases due to the decrement of concrete cover thickness.
6. It is noticed that the pullout failure is the predominant failure type observed on specimens for 12 mm and 14 mm bar diameter; however the specimens with 16 mm bar diameter failed with splitting failure.
7. The bond stress-slip curves of the SSA concrete specimens are almost similar to the bond stress-slip curve of the conventional aggregate concrete specimens; however the bond stress-slip curve of pullout failed specimens are different form the splitting failed specimens.
8. The proposed empirical equation for ultimate bond strength is a function of the compressive strength, concrete cover thickness, and bar diameter, which yields compatible bond strength values with Chapman and Shah empirical equation, and Huang et al. model code equation.

5.2 Recommendations

Due to the limitation of laboratory test machine and equipment, the pullout test was conducted on cylindrical specimens with centrally fixed deformed steel bar.

- ✓ It recommends that use of another bond strength test methods like beam-end specimen test to investigate the bond behavior of steel slag aggregate concrete for the future study.
- ✓ The Long time effect of steel slag on the bond strength of reinforced concrete such as the cause of corrosion needs investigation for the future study.
- ✓ The effect of the other bond strength parameters, like bar rib height, rib type, and embedment length with steel slag aggregate needs investigation.

REFERENCES

[1] Motz, H. and Geiseler, J., 2001. Products of steel slags an opportunity to save natural resources. *Waste management*, *21*(3), pp.285-293.

[2] Faleschini, F., De Marzi, P. and Pellegrino, C., 2014. Recycled concrete containing EAF slag: environmental assessment through LCA. *European journal of environmental and civil engineering*, *18*(9), pp.1009-1024.

[3] Subramani, T. and Ravi, G., 2015. Experimental investigation of coarse aggregate with steel slag in concrete. *IOSR Journal of Engineering*, *5*(5), pp.64-73.

[4] Pellegrino, C. & Faleschini, F. 2013. Experimental behavior of reinforced concrete beams with electric arc furnace slag aggregate. *ACI Material Journal,* 110-2: 197-205.

[5] Faleschini, F., Santamaria, A., Zanini, M.A., San José, J.T. and Pellegrino, C., 2017. Bond between steel reinforcement bars and Electric Arc Furnace slag concrete. *Materials and Structures*, *50*(3), p.170.

[6] Darwin, D., Dolan, C.W. and Nilson, A.H., 2016. *Design of concrete structures* (Vol. 2). New York, NY, USA:: McGraw-Hill Education

[7] Bond, A.C.I., 2003. Development of Straight Reinforcing Bars in Tension. *ACI 408R-03.*

[8] Papayianni, I. & Anastasiou, E. 2010. Production of high-strength concrete using high volume of industrial by-products. *Construction and Building Materials* 24: 1412 – 1417.

[9] Padmapriya, R., Bupesh Raja, V.K., Kumar, V.G. and Baalamurugan, J., 2015. Study on replacement of coarse aggregate by steel slag and fine aggregate by manufacturing sand in concrete. *International Journal of ChemTech Research, 8*(4), pp.1721-1729.

[10] Schoenberger, H., 2001. Final draft: best available techniques reference document on the production of iron and steel. *Publications of EC: European Commission, Joint Research Centre, IPTS, European IPPC Bureau*.

[11] Luxán, M.P.D., Sotolongo, R., Dorrego, F. and Herrero, E., 2000. Characteristics of the slags produced in the fusion of scrap steel by electric arc furnace. *Cement and concrete Research*, *30*(4), pp.517-519.

[12] Rainova, A., Seps, K. and Vytlacilova, V., 2012. Possible use of the slag aggregate in fibre reinforced concrete. In *Proceedings of Metal 2012 (21st International Conference on Metallurgy and Materials)*.

[13] Devi, V.S. and Gnanavel, B.K., 2014. Properties of concrete manufactured using steel slag. *Procedia Engineering*, *97*, pp.95-104.

[14] Warudkar, A.A. and Nigade, Y.M., 2015. Technical Assessment on Performance of Partial Replacement of Coarse Aggregate by Steel Slag in Concrete. *International Journal of Engineering Trends and Technology (IJETT)*–Volume, 30.

[15] Van Tran, M., Van Nguyen, C., Nawa, T. and Stitmannaithum, B., 2015. Properties of high strength concrete using steel slag coarse aggregate. *ASEAN Engineering Journal*, *4*(2), pp.22-32.

[16] Faleschini, F., Fernández-Ruíz, M.A., Zanini, M.A., Brunelli, K., Pellegrino, C. and Hernández-Montes, E., 2015. High performance concrete with electric arc furnace slag as aggregate: Mechanical and durability properties. *Construction and Building Materials*, 101, pp.113-121.

[17] Tastani, S.P. and Pantazopoulou, S.J., 2009. Direct tension pull-out bond test: Experimental Results, *Journal of Structural Engineering*, vol. 6, no. 136. pp. 731–743.

[18] Abrams, D.A., 1913. *Tests of bond between concrete and steel*. University of Illinois at Urbana Champaign, College of Engineering. Engineering Experiment Station.

[19] Wight, J. and MacGregor, J.G., 2009. Reinforced concrete. Mechanics and Design. (5a ed.) EEUU: Pearson.

[20] Shima, H., Chou, L.L. and Okamura, H., 1987. Micro and macro models for bond in reinforced concrete. *Journal of the Faculty of Engineering*, *39*(2), pp.133-194.

[21] Lundgren, K., 2005. Bond between ribbed bars and concrete. Part 1: Modified model. *Magazine of concrete research*, *57*(7), pp.371-382.

[22] Eligehausen, R., Popov, E.P., Bertero, V.V., 1983. Local Bond Stress-Slip Relationships of Deformed Bars under Generalized Excitations. Berkeley, CA, USA: University of California.

[23] Oh, B.H. and Kim, S.H., 2007. Realistic models for local bond stress-slip of reinforced concrete under repeated loading. *Journal of Structural Engineering*, *133*(2), pp.216-224.

[24] Filippou, F.C., Popov, E.P. and Bertero, V.V., 1983. Modeling of R/C joints under cyclic excitations. *Journal of Structural Engineering*, 109(11), pp.2666-2684.

[25] Huang, Z., Engström, B. and Magnusson, J., 1996, May. Experimental and analytical studies of the bond behaviour of deformed bars in high strength concrete. In *4th International Symposium on the Utilization of High Strength/High Performance Concrete* (Vol. 3).

[26] Code, M., 2010. FIB model Code for concrete structures. *Committee Euro-International du Beton, Lausanne, Switzerland.*

[27] Lutz, L.A. and Gergely, P., 1967, November. Mechanics of bond and slip of deformed bars in concrete. In *Journal Proceedings* (Vol. 64, No. 11, pp. 711-721).

[28] Lee, B. and Mulheron, M., 2012. Fluctuation of bond stress–slip behaviour of deformed bar under displacement control. *Magazine of concrete research*, *64*(10), pp.863-875.

[29] Harajli, M.H., Hout, M. and Jalkh, W., 1995. Local bond stress-slip behavior of reinforcing bars embedded in plain and fiber concrete. *Materials Journal*, *92*(4), pp.343-353.

[30] Ferguson, P.M., 1977, September. Small bar spacing or cover a bond problem for the designer. In *Journal Proceedings* (Vol. 74, No. 9, pp. 435-439).

[31] Rehm, G. and Eligehausen, R., 1979. Bond of ribbed bars under high cycle repeated loads. *ACI journal, Proceedings* (V. 76, No. 2, Feb., pp. 297-309).

[32] Iqbal, S., Ullah, N. and Ali, A., 2018. Effect of Maximum Aggregate Size on the Bond Strength of Reinforcements in Concrete. *Engineering, Technology & Applied Science Research*, *8*(3), pp.2892-2896.

[33] RILEM T.C., 1194. Bond test for reinforcement steel. 2. Pull-out test, in RILEM (Ed.), RILEM Recommendations for the Testing and Use of Constructions Materials, *E & FN SPON*, pp. 218–220.

[34] Ministry of Urban Development & Construction, 2015. Design of Concrete Structures, *ESEN 1992-1-1*, pp. 139–143.

[35] ACI Committee, 2008. Building code requirements for structural concrete (ACI 318- 08) and commentary. American Concrete Institute.

[36] Orangun, C.O., Jirsa, J.O. and Breen, J.E., 1977, March. A reevaluation of test data on development length and splices. In *Journal Proceedings* (Vol. 74, No. 3, pp. 114 122).

[37] Darwin, D., McCabe, S.L., Idun, E.K. and Schoenekase, S.P., 1992. Development length criteria: bars not confined by transverse reinforcement. American Concrete Institute.

[38] Chapman, R.A. and Shah, S.P., 1987. Early-age bond strength in reinforced concrete. *Materials Journal, 84*(6), pp.501-510.

[39] Aslani, F. and Nejadi, S., 2012. Bond behavior of reinforcement in conventional and self-compacting concrete. *Advances in Structural Engineering, 15*(12), pp.2033-2051.

[40] Dinku, A., 2002. Construction Material Laboratory Manual. Civil Engineering Department, Addis Ababa University, Ethiopia

[41] ASTM, C-125, 2003. Standard terminology relating to concrete and concrete aggregates, 1-4 S. *ASTM International, Conshohocken*.

[42] ASTM, C-33, 2003. Standard specification for concrete aggregates. Philadelphia, PA: American Society, *Testing and Materials*

[43] Dixon, D.E., Prestrera, J.R., Burg, G.R., Chairman, S.A., Abdun-Nur, E.A., Barton, S.G., Bell, L.W., Blas Jr, S.J., Carrasquillo, R.L., Carrasquillo, P.M. and Carter, A.C., 1991. Standard Practice for Selecting Proportions for Normal, Heavyweight, and Mass Concrete (ACI 211.1-91). Farmington Hills, MI, USA: American Concrete Institute.

[44] ASTM, C-192, 2002. Standard Practice for Making and Curing Concrete Test Specimens in the Laboratory, *Annual Book of ASTM Standards*, vol. 04. pp. 1–8.

[45] ASTM, C-143, 2008. Standard Test Method for Slump of Hydraulic-Cement Concrete, *Annual Book of ASTM Standards*, vol. 04, no. 02. pp. 1–3.

[46] ASTM International Committee C09 on Concrete and Concrete Aggregates, 2014. *Standard test method for compressive strength of cylindrical concrete specimens*. ASTM international.

[47] ASTM, C., 2011. Standard test method for splitting tensile strength of cylindrical concrete specimens. *C496/C496M-11*.

[48] Tang, C.W. and Cheng, C.K., 2020. Modeling Local Bond Stress–Slip Relationships of Reinforcing Bars Embedded in Concrete with Different Strengths. *Materials*, *13*(17), p.3701.

[49] Ogura, N. and Ichinose, T., 2004. Analytical study on splitting bond failure of deformed bars. *Journal of Structural and Construction Engineering*, (586), pp.147-154.

APPENDIX

Appendix A - Physical property tests for Fine Aggregate, Coarse Aggregate and Steel Slag Aggregate

Appendix B - Mix Design

Appendix C - Mechanical Properties of Reinforcement Bar

Appendix D - Test results for Compressive strength of concrete

Appendix E - Test results for splitting tensile strength of concrete

Appendix F - Test Results for Pull-out bond strength test

Appendix G - Sample Photos

Appendix H - Chemical composition of the steel slag

Appendix A - Physical property tests for Fine Aggregate, Coarse Aggregate and Steel Slag Aggregate

A-1: Tests for Fine Aggregate

1. Moisture content

Weight of sample = 500 g

Weight of oven-dry sample = 477.8 g

$$\text{Moisture content}(\%) = \frac{\text{Original sample weight} - (\text{ Oven dry weight})}{\text{Oven dry Weight}} \times 100$$

$$\text{Moisture content}(\%) = \frac{500\text{ g} - 477.8\text{ g}}{477.8\text{ g}} \times 100 = 4.65\%$$

2. Specific gravity of fine aggregate

Weight of sample = 500 g

Weight of pycnometer + water = 706.4 g

Weight of pycnometer + water + sample = 1007.1 g

Weight of oven-dry sample = 488.9 g

$$\text{Bulk specific gravity} = \frac{488.9}{706.4 + 500 - 1007.1} = 2.45$$

$$\text{Bulk specific gravity (SSD)} = \frac{500}{706.4 + 500 - 1007.1} = 2.51$$

$$\text{Apparent specific gravity} = \frac{488.9}{706.4 + 488.9 - 1007.1} = 2.60$$

$$\text{Water absorption }(\%) = \frac{500 - 488.9}{488.9} \times 100 = 2.27\%$$

3. Sieve analysis of fine aggregate

Sieve size (mm)	Weight Retained (g)	Percent of retained	Percent of Cumulative retained	Percent of Cumulative passing	ASTM C33 standard passing (%)
9.5	0	0	0	100	100
4.75	0.6	0.12	0.12	99.88	95-100
2.36	21.9	4.38	4.5	95.5	80-100
1.18	69.8	13.96	18.46	81.54	50-85
0.6	177.8	35.56	54.02	45.98	25-60
0.3	201.9	40.38	94.4	5.6	5-30
0.15	25.9	5.18	99.58	0.42	0-10
Pan	2.1	0.42	100	0	0

$$\text{Fineness modulus } = \frac{\sum(\text{cumulative percent of retained})}{100} = \frac{271.08}{100} = 2.71$$

A-2: Tests for Natural Coarse Aggregate

1. Moisture content of coarse aggregate

Weight of sample = 2000 g

Weight of oven-dry sample = 1974.7 g

$$\text{Moisture content}(\%) = \frac{\text{Original sample weight} - (\ \text{Oven dry weight})}{\text{Oven dry Weight}} \times 100$$

$$\text{Moisture content}(\%) = \frac{2000\ \text{g} - 1974.7\ \text{g}}{1974.7\ \text{g}} \times 100 = 1.28\%$$

2. Unit weight of coarse aggregate

Mass of Apparatus = 4.85 kg

Mass of Apparatus + sample = 26.84 kg

Volume of Apparatus = 0.014 m^3

$$\text{Unit weight} = \frac{27.65\ \text{kg} - 4.85\ \text{kg}}{0.014\ \text{m}^3} = 1570.71\ \text{kg/m}^3$$

3. Specific gravity of coarse aggregate

A = Weight of oven dry sample (OD) = 4888 g

B = Weight of saturated surface dry (SSD) = 4950 g

C = Weight of saturated sample in water = 3124.9 g

$$\text{Bulk specific gravity} = \frac{A}{B - C} = \frac{4888\ \text{g}}{4950\ \text{g} - 3124.9\ \text{g}} = 2.68$$

$$\text{Bulk specific gravity (SSD)} = \frac{B}{B - C} = \frac{4950\ \text{g}}{4950\ \text{g} - 3124.9\ \text{g}} = 2.71$$

$$\text{Apparent specific gravity} = \frac{A}{A - C} = \frac{4888\ \text{g}}{4888\ \text{g} - 3124.9\ \text{g}} = 2.77$$

$$\text{Water absorption Capacity (\%)} = \frac{B - A}{A} \times 100 = \frac{4950\ \text{g} - 4888\ \text{g}}{4888\ \text{g}} \times 100 = 1.27\%$$

4. Sieve analysis of coarse aggregate

Sieve size (mm)	Weight Retained (g)	Percent of retained	Percent of Cumulative retained	Percent of Cumulative passing	ASTM C33 standard passing (%)
25	0	0	0	100	95-100
19	231.2	11.56	11.56	88.44	-
12.5	882	44.1	55.66	44.34	25-60
9.5	636.2	31.81	87.47	12.53	-
4.75	247	12.35	99.82	0.18	0-10
Pan	3.6	0.18	100	0	0

Fineness modulus of coarse aggregate is calculated by sum up of the percentage cumulative retained for sieve size of (38.1 mm, 19 mm, 9.5 mm, 4.75 mm, 2.36 mm,1.18 mm, 0.6 mm, 0.3 mm and 0.15 mm) divided by 100.

Sieve size (mm)	Cumulative coarser (%)
38.1	0
19	11.56
9.5	87.47
4.75	99.82
2.36	100
1.18	100
0.6	100
0.3	100
0.15	100

Σ(% Cumulative retained) = 698.85

$$\text{Fineness modulus} = \frac{\sum(\text{Cumulative percent of retained})}{100} = \frac{698.85}{100} = 6.99$$

A-3: Tests for Steel Slag Aggregate

1. Moisture content of steel slag aggregate

Weight of sample = 2000 g

Weight of oven-dry sample =1979.5 g

$$\text{Moisture content}(\%) = \frac{\text{original sample weight} - (\text{ oven dry weight})}{\text{oven dry Weight}} \times 100$$

$$\text{Moisture content}(\%) = \frac{2000\text{ g} - 1979.5\text{ g}}{1979.5\text{ g}} \times 100 = 1.04\%$$

2. Unit weight of steel slag aggregate

Mass of apparatus = 4.85 kg

Mass of apparatus + sample = 24.01 kg

Volume of apparatus = 0.014 m^3

$$\text{unit weight} = \frac{24.01\text{ kg} - 4.85\text{ kg}}{0.014\text{ m}^3} = 1368.57\text{ kg/m}^3$$

3. Specific gravity of steel slag aggregate

A = Weight of oven dry sample (OD) = 4908.8 g

B = Weight of saturated surface dry (SSD) = 5014.2 g

C = Weight of saturated sample in water = 2926.1 g

$$\text{Bulk specific gravity} = \frac{A}{B - C} = \frac{4908.8\text{ g}}{5014.2\text{ g} - 2926.1\text{ g}} = 2.35$$

$$\text{Bulk specific gravity (SSD)} = \frac{B}{B - C} = \frac{5014.2\text{ g}}{5014.2\text{ g} - 2926.1\text{ g}} = 2.40$$

$$\text{Apparent specific gravity} = \frac{A}{A - C} = \frac{4908.8\text{ g}}{4908.8\text{ g} - 2926.1\text{ g}} = 2.48$$

$$\text{Water absorption Capacity (\%)} = \frac{B - A}{A} \times 100 = \frac{5014.2\text{ g} - 4908.8\text{ g}}{4908.8\text{ g}} = 2.15\%$$

4. Sieve analysis of steel slag aggregate

Sieve size (mm)	Weight Retained (g)	Percent of retained (%)	Cumulative retained (%)	Cumulative passing (%)	ASTM C33 standard passing (%)
25	0	0	0	100	95-100
19	293.7	14.69	14.69	85.31	-
12.5	981.8	49.09	63.78	36.22	25-60
9.5	414.6	20.73	84.51	15.49	-
4.75	292.3	14.62	99.13	0.87	0-10
Pan	17.6	0.87	100	0	0

Fineness modulus of steel slag aggregate is calculated by sum up of the percentage cumulative retained for sieve size of (38.1 mm, 19 mm, 9.5 mm, 4.75 mm, 2.36 mm,1.18 mm, 0.6 mm, 0.3 mm and 0.15 mm) divided by 100.

Sieve size (mm)	**Cumulative retained (%)**
38.1	0
19	14.69
9.5	84.51
4.75	99.13
2.36	100
1.18	100
0.6	100
0.3	100
0.15	100

Σ(% Cumulative retained) = 698.33

$$\text{Fineness modulus} = \frac{\sum(\text{Cumulative percent of retained})}{100} = \frac{698.33}{100} = 6.98$$

Appendix B - Mix Design

Mix Design for C-30

Step 1. Material property

No	Tests	cement	Fine aggregate	Natural coarse aggregate	Steel slag aggregate
1	Specific gravity	3.15	2.45	2.68	2.35
2	Unit weight	-	1490.97kg/m^3	1570.71 kg/m^3	1368.57 kg/m^3
3	Moisture content	-	4.65%	1.28%	1.04%
4	Water absorption	-	2.27%	1.27%	2.15%
5	Fineness modulus	-	2.71	6.99	6.98

Step 2. Choice the slump

From the recommended slump value of ACI 211 Table 6.3.1, to address the most common constructions of concrete it considered beams, reinforced walls and columns with the slump ranges (25- 100) mm, minimum slump = 25 mm and maximum slump = 100 mm.

Step 3. Choice the maximum aggregate size

Fine aggregate = 4.75 mm

Coarse aggregate = 25 mm

Step 4. Estimation of Mixing water & Air content

Considered non-air-entrained concrete, from ACI 211 table 6.3.3, for non-air entrained and slump of 25-50 and also for maximum aggregate size = 25 mm, the water in 1 m^3 of concrete is 179 Kg and the entrapped air content is 1.5%.

Step 5. Water-Cement ratio (W/C)

The water to cement ratio for the required compressive strength of 38 MPa is 0.44

W/C = 0.44

Step 6. Cement content calculation

Water content = 179 kg

w/c = 0.44

Cement content (Kg) for 1 m^3 of concrete = $\frac{179kg}{0.44} = 406.82\ kg$

Step 7. Estimation of Coarse aggregate (CA) content

From ACI table 6.3.6, for fineness modulus of fine aggregate = 2.71 and Maximum aggregate Size of coarse aggregate = 25 mm the volume of dry-rodded coarse aggregate per unit volume of concrete is 0.68.

Coarse aggregate content = 0.68 × 1570.71 kg/m^3 = 1068.08 kg

Step 8. Estimation of Fine aggregate content

By absolute volume method

In absolute volume method the volume of fine aggregate is determined by subtracting the volume of all known ingredients from unit volume of concrete.

$$\text{Volume} = \frac{\text{mass(kg)}}{\text{specific gravity} \times \text{density of water}}$$

$$\text{Volume of Water} = \frac{179}{1 \times 1000} = 0.179 \text{ m}^3$$

$$\text{Volume of Cement} = \frac{406.82}{3.15 \times 1000} = 0.129 \text{ m}^3$$

$$\text{Volume of Coarse aggregate} = \frac{1068.08}{2.68 \times 1000} = 0.399 \text{ m}^3$$

Volume of air = 1.5%

Therefore -

Volume of fine aggregate = unit volume of concrete - volume of (coarse aggregate + cement + water + air)

= 1 – (0.399 + 0.129 + 0.179 + 0.015) = 0.28 m3

Mass of fine aggregate = 0.28 × 2.45 × 1000 = 686.0 kg

Adjusted mass of fine aggregate = 686.0 kg + (4.65% × 686 kg) = 717.90 kg

Step 9. Moisture adjustment

If the moisture content of aggregate is greater than the water absorption capacity of it, we need reduce the mixed added water to get better workability of the concrete.

C.A reduced water = 1.28 -1.27 = 0.01%

SSA reduced water = 1.04 -2.15 = -1.11%

F.A reduced water = 4.65 -2.27 = 2.38%

Total required water = 179 - ((mass C.A ×0.01%) + (mass F.A×2.38%) + (mass of SSA ×-1.11%))

Total required water = 179 - ((1068.08 ×0.01%) + (717.90×2.38%) +0) = 161.81 kg, for SSA-0

Content of ingredients for unit volume of concrete for SSA-0

No	Ingredients	Weight per unit volume (kg/m^3)
1	Cement	406.82
2	Fine aggregate	717.90
3	Coarse aggregate	1068.08
4	Water	161.81

- The replacement of coarse aggregate with SSA is by Volume replacement

Mass of steel slag aggregate = (%) ×C.A volume ×specific gravity of SSA ×1000

Like, SSA 100 = 100% × 0.399 ×2.35 ×1000 = 937.65 kg

No	Ingredients	Weight per unit volume (kg/m^3)				
		(SSA-0)	(SSA-25)	(SSA-50)	(SSA-75)	(SSA-100)
1	Cement	406.82	406.82	406.82	406.82	406.82
2	Fine aggregate	717.90	717.90	717.90	717.90	717.90
3	Coarse aggregate	1068.08	801.06	534.04	267.02	0
4	Steel slag aggregate	0	234.41	468.83	703.24	937.65
5	Water	161.81	164.44	167.06	169.69	172.32

Step 10. Trial batch

Six cubes which are 150x150x150 mm, six cylinders with a diameter of 150 mm by a height of 300 mm and nine cylinders are required for compressive strength test, tensile strength test and pull-out test respectively for each mix. Having total volume of 0.0998 m^3 per mix.

Consider 15% wastage = 0.15 × 0.0998 m3 = 0.015 m3

Total volume = 0.0998 +0.015 = 0.1148 m3, due to the volume is larger than laboratory mixer capacity it is mixed in two round.

Ingredients' content for each concrete mixes

No	**Ingredients**	**Weight (kg)**				
		m-1 (SSA-25)	**m-2 (SSA-25)**	**m-3 (SSA-50)**	**m-4 (SSA-75)**	**m-5 (SSA-100)**
1	Cement	46.70	46.70	46.70	46.70	46.70
2	Fine aggregate	82.41	82.41	82.41	82.41	82.41
3	Coarse aggregate	122.62	91.96	61.31	30.65	0
4	Steel slag aggregate	0	26.91	53.82	80.73	107.64
5	water	18.58	18.88	19.18	19.48	19.78

Appendix C - Mechanical Properties of Reinforcement Bar

Specimen No	Diameter		Av. Diameter (mm)	Area (mm)	Yield Load (KN)	Failure Load (KN)	Elongation (%)	Mass/length (Kg/m)	Length (cm)	Yield Strength (Mpa)	Ultimate strength (Mpa)	Av. Yield Strength (Mpa)	Av. Ultimate strength (Mpa)
	D_1, (mm)	D_2, (mm)											
12-1	11.47	12.64	12.055	114.14	74.2	85.7	23	866.9	100	650.08	750.83	654.38	755.4
12-2	11.42	12.66	12.04	113.85	74.7	86.2	23.2	862.9	100	656.13	757.14		
12-3	11.4	12.69	12.045	113.95	75.2	86.4	23.2	868.1	100	656.94	758.23		
14-1	13.47	14.72	14.095	156.03	88.4	106.1	23.1	1174.7	100	566.56	680	559.07	672.81
14-2	13.49	14.74	14.115	156.48	87.4	105.9	22.9	1176.8	100	558.54	676.76		
14-3	13.51	14.77	14.14	157.03	86.7	103.9	22.7	1224.7	101	552.12	661.66		
16-1	15.41	16.76	16.085	203.2	117.4	140.9	23	1252.2	81	577.76	693.41	581.29	701.04
16-2	15.34	16.74	16.04	202.07	118.2	143.2	22.9	1221.5	80	584.95	708.67		
16-3	15.38	16.75	16.065	202.7	117.8	142.1	23	1221.6	80	581.15	701.04		

Appendix D - Test results for Compressive strength of concrete

SSA(%)	Test age (Days)	Weight (gm)	Failure load (kN)	Compressive strength (MPa)	Average Compressive strength (MPa)
0	7	8329	699.3	31.08	31.12
		8464	696.6	30.96	
		8374	704.7	31.32	
	28	8391	990.9	44.04	43.46
		8355	961	42.71	
		8376	981.5	43.62	
25	7	8083	739.3	32.86	33.26
		8228	745.9	33.15	
		8209	759.9	33.77	
	28	8314	1014.9	45.1	45.68
		8338	1052.6	46.78	
		8135	1016.5	45.17	
50	7	7930	770.9	34.26	34.27
		7982	771.1	34.27	
		8120	771.5	34.29	
	28	8088	1095.3	48.68	47.98
		8074	1059.2	47.07	
		8156	1084.5	48.2	
75	7	7705	694	30.84	31.25
		7950	725.8	32.26	
		7703	689.6	30.65	
	28	7878	1001	44.49	43.24
		7877	947.5	42.11	
		7928	970.4	43.13	
100	7	7603	609.4	27.08	26.97
		7684	586.9	26.08	
		7533	624.2	27.74	
	28	7959	883.6	39.27	39.13
		7717	867	38.53	
		7753	891	39.6	

Appendix E - Test results for splitting tensile strength of concrete

SSA(%)	Test age (days)	Weight (gm)	Failure load (KN)	Splitting Tensile (MPa)	Average Splitting Tensile (MPa)
0	7	13151	217.71	3.08	3.03
		13273	210.64	2.98	
		13267	213.47	3.02	
	28	13095	302.54	4.28	4.11
		13103	288.4	4.08	
		13226	280.62	3.97	
25	7	12862	278.5	3.94	3.59
		12764	224.07	3.17	
		12848	258.71	3.66	
	28	12970	313.14	4.43	4.56
		12888	315.26	4.46	
		12986	337.88	4.78	
50	7	12581	241.75	3.42	3.63
		12572	265.78	3.76	
		12569	262.24	3.71	
	28	12536	345.65	4.89	4.76
		12,432	311.02	4.4	
		12542	352.02	4.98	
75	7	12135	221.25	3.13	3.06
		12220	210.64	2.98	
		12171	217.01	3.07	
	28	12154	284.16	4.02	4.16
		12155	307.48	4.35	
		12177	290.52	4.11	
100	7	11854	212.76	3.01	3.02
		11670	209.94	2.97	
		11865	217.01	3.07	
	28	11872	266.49	3.77	4.14
		11788	325.86	4.61	
		11879	286.28	4.05	

Appendix F - Test Results for Pull-out bond strength test

Specimen	Diameter of bar (mm)	Failure load (KN)	Average failure load (KN)	Bond Stress (MPa)	Average bond Stress (MPa)	Free end Slip (mm)	Average slip (mm)	Failure mode
SSA-0	12	40.1	41.83	17.73	18.49	0.88	0.98	Pullout
		43.6		19.28		1.23		Pullout
		41.8		18.48		0.84		Pullout
	14	52.8	51.27	17.15	16.65	0.96	1.16	Pullout
		49.9		16.21		1.24		Pullout
		51.1		16.60		1.28		Pullout
	16	65.4	66.33	16.26	16.5	0.56	0.39	Splitting
		66.7		16.59		0.42		Splitting
		66.9		16.64		0.19		Splitting
SSA-25	12	43.1	45.43	19.05	20.09	1.02	0.95	Pullout
		46.1		20.38		1.32		Pullout
		47.1		20.82		0.51		Pullout
	14	51.8	51.6	16.83	16.76	1.34	1.12	Pullout
		52.4		17.02		1.04		Pullout
		50.6		16.44		0.98		Pullout
	16	72.7	71.17	18.08	17.7	0.35	0.65	Splitting
		70.9		17.63		0.88		Splitting
		69.9		17.38		0.72		Splitting
SSA-50	12	42.6	43.1	18.83	19.05	0.98	0.88	Pullout
		42.9		18.97		0.65		Pullout
		43.8		19.36		1.01		Pullout
	14	57.3	56.97	18.61	18.5	1.12	1.05	Pullout
		54.4		17.67		0.95		Pullout
		59.2		19.23		1.08		Pullout
	16	69.2	71.33	17.21	17.74	0.74	0.51	Splitting
		71.6		17.81		0.5		Splitting

		73.2		18.20		0.27		Splitting
SSA-75	12	36.4	38.57	16.09	17.05	0.79	0.96	Pullout
		41.4		18.30		1.08		Pullout
		37.9		16.76		1.01		Pullout
	14	51.4	51.73	16.70	16.8	1.95	1.56	Pullout
		50.4		16.37		1.58		Pullout
		53.4		17.34		1.15		Pullout
	16	64.2	65.8	15.97	16.36	0.37	0.57	Splitting
		65.8		16.36		0.66		Splitting
		67.4		16.76		0.68		Splitting
SSA-100	12	38.6	37.35	17.07	16.51	1.38	1.32	Pullout
		36.1		15.96		1.26		Pullout
	14	50.8	49.07	16.50	15.94	1.55	1.55	Pullout
		49.1		15.95		1.75		Pullout
		47.3		15.36		1.35		Pullout
	16	62.9	63.2	15.64	15.72	0.44	0.49	Splitting
		61.9		15.39		0.5		Splitting
		64.8		16.11		0.54		Splitting

Appendix G - Sample Photos

Steel Slag at Kalti Metal Production Industry

Sieving of steel slag aggregate

Aggregate impact test for SSA

Ingredients ready for mixing

Concrete casting

Curing of concrete member specimens

Specimens for pullout test

Pullout bond strength test

pullout Bond failure

Splitting Bond failure

Appendix H - Chemical composition of the steel slag

	GEOLOGICAL SURVEY OF ETHIOPIA	Doc.Number: GLD/F5.10.2	Version No: 1
	GEOCHEMICAL LABORATORY DIRECTORATE		Page 1 of 1
Document Title:	Complete Silicate Analysis Report	Effective date:	May, 2017

Issue Date: -04/06/2021

Customer Name:-Melkam Gubay Ejigu

Request No:- GLD/RQ/958/21

Report No:- GLD/RN/505/21

Sample type :-Soil

Sample Preparation: - 200 Mesh

Date Submitted :-27/04/2021

Number of Sample:- One(01)

Analytical Result: In percent (%) Element to be determined Major Oxides & Minor Oxides

Analytical Method: $LiBO_2$ FUSION, HF attack, GRAVIMETERIC, COLORIMETRIC and AAS

Collector's code	SiO_2	Al_2O_3	Fe_2O_3	CaO	MgO	Na_2O	K_2O	MnO	P_2O_5	TiO_2	H_2O	LOI
Steel Slag	55.62	14.18	10.94	1.36	1.08	0.56	3.44	11.26	0.07	0.54	0.26	<0.01

Note: - This result represent only for the sample submitted to the laboratory.

Analysts	Checked By	Approved By	Quality Control
Lidet Endeshaw			
Yirgalem Abreham	Tizita Zemene	Yohannes Getachew	Gesa Haile
Nigist Fikadu			